

Magnetically-driven jets from Keplerian accretion discs

Jonathan Ferreira

Landessternwarte, Königstuhl, D-69117 Heidelberg, Germany
jferreir@lsw.uni-heidelberg.de

Received March 30; accepted July 2, 1996

Abstract. Non-relativistic, magnetically-driven jets are constructed by taking self-consistently into account the feedback on the underlying accretion disc. It is shown that such jets are mostly described by the ejection index $\xi = d \ln M_a / d \ln r$, which is a local measure of the disc ejection efficiency. This parameter is found to lie in a very narrow range, due to constraints imposed by both the disc vertical equilibrium and the steady transfer of angular momentum.

The investigation of global disc-jets solutions provided two important results. First, it shows that the disc vertical equilibrium imposes a minimum mass flux ejected. Thus, one cannot construct jet models with arbitrarily small mass loads. Second, their asymptotic behaviour critically depends on a fastness parameter $\omega_A = \Omega_* r_A / V_{Ap,A}$, ratio of the field lines rotation velocity to the poloidal Alfvén velocity at the Alfvén surface. This parameter must be bigger than, but of the order of, unity.

Self-similar jets from Keplerian discs, after widening up to a maximum radius whose value increases with ω_A , always recollimate towards the jet axis, until the fast-magnetosonic critical point is reached. It is doubtful that such solutions could steadily cross this last point, the jet either ending there or rebouncing. Recollimation takes place because of the increasing effect of magnetic constriction. This systematic behaviour is due to the large opening of the magnetic surfaces, leading to such an efficient acceleration that matter always reaches its maximum poloidal velocity. This “over-widening” stems from having the same ejection efficiency ξ in the whole jet.

Realistic jets, fed with ejection indices varying from one magnetic surface to the other, would not undergo recollimation, allowing either cylindrical or parabolic asymptotic collimation. The study of such jets requires full 2-D numerical simulations, with proper boundary conditions at the disc surface.

Key words: Accretion, accretion discs – Magnetohydrodynamics (MHD) – Stars: formation – ISM: jets and outflows – Galaxies: nuclei – Galaxies: jets

1. Introduction

It is now widely accepted that accretion of matter onto a central object plays a major role in astrophysics: in active galactic nuclei (AGN), young stellar objects (YSOs), but also in evolved binary systems like cataclysmic variables or low-mass X-ray binaries.

The standard theory of accretion discs (Shakura & Sunyaev 1973, Novikov & Thorne 1973, Lynden-Bell & Pringle 1974) assumes the presence of a turbulent viscosity that allows the matter to loose its angular momentum and mechanical energy. This energy is then radiated away at the disc surfaces, providing the observed luminosity (e.g., Bregman 1990, Bertout et al. 1988). However, such a theory is unable to explain the origin, acceleration and collimation of bipolar jets, that are emanating from radio loud AGN and quasars (Bridle & Perley 1984), all YSOs (Lada 1985) and some galactic objects like SS 433, Sco X-1 (Padman et al. 1991) and “microquasars” (Mirabel et al. 1992).

In the vicinity of a black hole, the jet plasma has to come from a surrounding accretion disc. Lynden-Bell (1978) suggested that in the framework of a thick accretion disc, jets could be produced in the inner funnel around the axis of the torus, and accelerated like in a De Laval nozzle. Such a thick torus could be either radiation-supported (with a super-Eddington accretion rate, e.g. Abramowicz et al. 1980), or ion-supported (with a sub-critical accretion rate, Rees et al. 1982). Jets would then be accelerated by radiation pressure (Abramowicz & Piran 1980) or by the rotational energy of the central black hole (Blandford & Znajek 1977). This latter process, unique possibility within the second scenario, invokes a large scale magnetic field dragged in by the disc, braking the fastly rotating hole and transferring its energy to matter (see also Phinney 1983). However, it has been shown that such thick tori are violently unstable (Papaloizou & Pringle 1984, Zurek & Benz 1986, Begelman et al. 1987), casting therefore strong doubts upon their viability to produce jets.

The remaining scenario invokes a large scale magnetic field, anchored on a geometrically thin (Keplerian) ac-

cretion disc (Blandford & Payne 1982, hereafter BP82). These authors showed that this magnetic field could brake the disc and carry away its angular momentum. If jets carry a current, then the toroidal component of the magnetic field would provide a tension that naturally confines the jet (previously recognized by Chan & Henriksen 1980).

For protostars, the situation is more complex, since the observed jets could be either stellar winds (Canto 1980, Hartmann et al. 1982, Lago 1984) or disc winds (Pudritz & Norman 1983, Uchida & Shibata 1985). However, both mass and momentum fluxes of the observed outflows are much higher than the ones provided by the protostar luminosity, hence forbidding both thermally and radiation pressure driven stellar winds (DeCampli 1981, Königl 1986). The possibility remains that stellar magnetic fields play a major role in producing a wind (Messtel 1968, Hartmann & MacGregor 1982, Sakurai 1985, Tsinganos & Trussoni 1991, Sauty & Tsinganos 1994). But the strongest argument in favour of disc-driven jets is certainly the observed correlation between signatures of accretion and ejection (Cabrit et al. 1990, Hartigan et al. 1995).

To summary, one can conclude that both observational and theoretical investigations tend to show that, in order to produce powerful self-collimated jets, one has to rely on an accretion disc and a large scale magnetic field. Of course, the possibility that jets arise from the interaction between the central object magnetosphere and the disc has still to be worked out (Camenzind 1990, Shu et al. 1994). Nevertheless, the study of such an interaction requires first the deep understanding of the interplay between accretion and ejection processes. Hereafter, we call Magnetized Accretion-Ejection Structures (MAES), objects where these two processes are interdependent.

There have been a number of studies of magnetized jets in the past (BP82, Camenzind 1986, Lovelace et al. 1987, Heyvaerts & Norman 1989, Chiueh et al. 1991, Pelletier & Pudritz 1992, Li et al. 1992, Appl & Camenzind 1993a, Rosso & Pelletier 1994, Contopoulos 1995, to cite only a few), but all these works were focused on jet dynamics. Thus, it was not yet proved that the underlying disc could indeed provide the required boundary conditions.

Despite serious advances in the theory of magnetized accretion discs driving jets (Königl 1989, Ferreira & Pelletier 1993a, 1993b, 1995, Wardle & Königl 1993, Li 1995), this question has not yet been fully addressed. Indeed, in both Wardle & Königl and Li approaches, the disc solutions were obtained by not properly treating the disc vertical equilibrium and were directly matched to BP82's jet solutions (see Sect. 4.2.1). Moreover, by doing so, they were not able to specify the physical process leading plasma to change its radial motion (accretion) into a vertical one (ejection). Ferreira & Pelletier (1995, hereafter FP95) constructed disc solutions by taking into account all the dynamical terms, thus being able to answer this question, as well as derive the physical conditions re-

quired to magnetically launch jets. However, it remained to be proved that their solutions could indeed produce super-Alfvénic jets.

The goal of this paper is therefore to construct global, non-relativistic solutions for magnetically-driven jets from Keplerian discs. Our treatment allows a smooth transition between the resistive disc and the ideal MHD jet. This paper is organized as follows. We start by briefly recalling the MHD equations of MAES and their main features. In particular, we expose some general results on the physical processes that govern the disc. Section 3 is devoted to the properties of magnetically-driven jets and the constraints arising from their interplay with the underlying disc. Self-similar, non-relativistic solutions that smoothly cross both slow-magnetosonic and Alfvén critical points are displayed in Section 4. In the following section, we show the asymptotic behaviour of self-similar jets and investigate analytically the reason for their systematic behaviour. We conclude by summarizing our results in Section 6.

2. Keplerian accretion discs driving jets

2.1. Magnetohydrodynamic equations for MAES

In order to produce bipolar jets, it is natural to rely on a bipolar topology for the large scale magnetic field. The other alternative, a quadrupolar topology, could in principle be used too, but such a topology could only produce weak jets (if any, see Appendix A). In both cases, this large scale magnetic field has two distinct possible origins: advection of interstellar magnetic field with accreting matter or “in-situ” production through a disc dynamo (Pudritz 1981, Khanna & Camenzind 1994). Both scenarios raise unanswered questions. For example, on the degree of diffusion of the infalling matter, which strongly determines the field strength in the inner regions (Mouschovias 1991, FP95). On the other hand, dynamo theory is still kinematic and one cannot easily infer from these studies what would be the final stage of the magnetic topology, if the matter feedback on the field is taken into account (Yoshizawa & Yokoi 1993). Most probably, a realistic scenario would have to take into account advection of external magnetic field while its amplification by the local dynamo.

In what follows, we restrict ourselves to the bipolar topology and assume that this field, although it has a profound dynamical influence on the disc, is not strong enough to significantly perturb its radial balance. Thus, the disc is supposed to be geometrically thin (its half-width at a distance r verifies $h(r) \ll r$), in a quasi Keplerian equilibrium. The magnetohydrodynamic equations describing stationary, axisymmetric MAES are then the following:

$$\nabla \cdot \rho \mathbf{u} = 0 \quad (1)$$

$$\rho \mathbf{u} \cdot \nabla \mathbf{u} = -\rho \nabla \Phi_G - \nabla P + \mathbf{J} \times \mathbf{B} + \nabla \cdot \mathbf{T} \quad (2)$$

$$\mathbf{J} = \frac{1}{\mu_0} \nabla \times \mathbf{B} \quad (3)$$

$$\eta_m J_\phi = \mathbf{u}_p \times \mathbf{B}_p \quad (4)$$

$$\nabla \cdot \left(\frac{\nu'_m}{r^2} \nabla r B_\phi \right) = \nabla \cdot \frac{1}{r} (B_\phi \mathbf{u}_p - \mathbf{B}_p \Omega r) \quad (5)$$

where $\Phi_G = -GM/(r^2 + z^2)^{1/2}$ is the gravitational potential of the central object (disc self-gravity is neglected) and \mathbf{T} is a viscous stress tensor (Shakura & Sunyaev 1973). Both disc velocity and magnetic field were decomposed into poloidal and toroidal components, namely $\mathbf{u} = \mathbf{u}_p + \Omega r \mathbf{e}_\phi$ and $\mathbf{B} = \mathbf{B}_p + B_\phi \mathbf{e}_\phi$ respectively. A magnetic bipolar topology imposes an odd B_ϕ with respect to z , as well as a poloidal field

$$\mathbf{B}_p = \frac{1}{r} \nabla a \times \mathbf{e}_\phi, \quad (6)$$

where $a(r, z)$ is an even function of z . A magnetic surface, which is a surface of constant magnetic flux, is directly labelled by $a(r, z) = a_o(r_o, 0)$. The distribution of magnetic flux through the disc is a free (and unknown) function. We will therefore use a prescription consistent with the complete set of equations.

Since the magnetic field threads the disc, steady-state accretion requires that matter diffuses through the field. As usual in astrophysics, normal transport coefficients are far too small to account for the expected motions. Drift between ions and neutrals, known as ambipolar diffusion, could play such a role in accretion discs (Königl 1989, Wardle & Königl 1993). However, jets are observed in a wide variety of objects, which suggests that they are produced by a mechanism independent of the disc ionisation degree. Moreover, it is now well known that magnetized discs are prone to instabilities (e.g. Balbus & Hawley 1991, Tagger et al. 1992, Foglizzo & Tagger 1995, Curry & Pudritz 1995, Spruit et al. 1995). Thus, we assume that the disc is turbulent and that the non-linear evolution of this turbulence provides the required anomalous transport coefficients, such as the magnetic diffusivity ν_m , resistivity $\eta_m = \mu_0 \nu_m$ and viscosity ν_v (appearing in \mathbf{T}). All these transport coefficients should achieve a comparable level (Pouquet et al. 1976). Nevertheless, we introduced in Eq.(5) a “toroidal” magnetic diffusivity ν'_m to account for anisotropy with respect to the “poloidal” diffusivity ν_m . Indeed, the winding up of the field due to disc differential rotation can lead to strong instabilities and thus, to enhanced transport coefficients with respect to the toroidal field (see FP95).

Finally, in order to close the system, we use a polytropic approximation

$$P = \mathcal{K} \rho^\gamma \quad (7)$$

with \mathcal{K} constant along a magnetic surface, in the isothermal case ($\gamma = 1$). Magnetized jets driven by an accretion disc can be initially launched either by predominant magnetic effects (magnetically-driven) or by enthalpy alone

(thermally-driven). For discs without a hot corona (cold MAES with negligible enthalpy), FP95 showed that jets could indeed be produced through magnetic effects alone. For these magnetically-driven jets, the vertical profile of the temperature has not a strong influence on plasma dynamics, therefore allowing a description with an isothermal structure. The reason lies in the fact that most of the accretion power goes into the jets as an MHD Poynting flux. Thus, magnetically-driven jets will always be associated with weakly dissipative discs, where thermal effects can be neglected (see below).

Such a cold MAES corresponds to a “clean” magnetic structure at the disc surface, with just one polarity. In fact, it is likely that the magnetic structure would consist of open field lines coexisting with small scale loops anchored at different radii (Galeev et al. 1979, Heyvaerts & Priest 1989). Such a situation would then most probably result in the formation of a hot corona. The treatment of such a hot MAES is postponed to future work.

The local state of a cold MAES is mainly characterized by the set of following parameters evaluated at the disc midplane,

$$\begin{aligned} \varepsilon &= \frac{h}{r} \\ \mathcal{R}_m &= \frac{r u_r}{\nu_m} \\ \alpha_m &= \frac{\nu_m}{V_A h} \\ \mu &= \frac{B^2}{\mu_0 P} \\ \xi &= \frac{d \ln \dot{M}_a}{d \ln r} \\ \Lambda &= \frac{(\mathbf{J} \times \mathbf{B})_\phi}{(\nabla \cdot \mathbf{T})_\phi} \simeq \frac{2q\mu}{\alpha_v \varepsilon} \end{aligned} \quad (8)$$

namely, the disc aspect ratio $\varepsilon \ll 1$, the magnetic Reynolds number \mathcal{R}_m , the turbulence level parameter α_m , the disc magnetization μ , the ejection index $\xi > 0$ and the ratio Λ of the magnetic to the viscous torque (FP95). This ratio depends on the magnitude μ of the field, the magnetic shear q of order unity, defined as

$$q \equiv - \frac{h}{B_o} \left. \frac{\partial B_\phi}{\partial z} \right|_{z=0} \quad (9)$$

and being a measure of the toroidal field at the disc surface (Ferreira & Pelletier 1993a, hereafter FP93a) and, of course, on the magnitude of the viscosity through the well known α_v parameter (Shakura & Sunyaev 1973). Under the sole assumption that the disc is in Keplerian balance, angular momentum conservation implies that

$$1 + \Lambda \simeq \mathcal{R}_m \left(\frac{\nu_m}{\nu_v} \right)_{z=0} \quad (10)$$

must be verified at the disc midplane. If large scale magnetic fields are irrelevant ($\Lambda \ll 1$), one recovers that the

Reynolds number $\mathcal{R}_v = ru_r/\nu_v$ is of order unity, which is required in standard viscous discs. On the contrary, when they significantly brake the disc, one obtains that the degree of curvature of the field lines at the disc surface (measured by \mathcal{R}_m) depends mostly on how strong is Λ . BP82 showed that in order to magnetically launch jets without a hot corona, the magnetic structure needs to be bent by more than 30° with respect to the vertical axis. This implies a magnetic Reynolds number of order $\mathcal{R}_m \gtrsim \varepsilon^{-1}$, therefore $\Lambda \gtrsim r/h$. Cold jets require then a dominant magnetic torque, imposing a corresponding value on both the field strength and shear.

Energy conservation equation (FP93a),

$$P_{lib} = 2P_{rad} + 2P_{MHD} + 2P_{th} \quad (11)$$

shows that the total available mechanical power P_{lib} is shared by the disc luminosity P_{rad} , the outward MHD Poynting flux P_{MHD} and the flux of thermal energy P_{th} from each surface of the disc. The liberated power is such that $P_{lib} \lesssim P_{acc} \equiv GM\dot{M}_{ae}/2r_i$ (see FP95, Ferreira 1996), where r_i is the disc inner radius and \dot{M}_{ae} is the accretion rate at the disc outer edge r_e . Around a compact object, this accretion power is

$$P_{acc} \simeq 4.7 \cdot 10^{45} \left(\frac{\dot{M}_{ae}}{\dot{M}_*} \right) \left(\frac{r_i}{r_*} \right)^{-1} \text{ erg s}^{-1} \quad (12)$$

for $\dot{M}_* = 1M_\odot \text{yr}^{-1}$, $r_* = 3r_g$, where $r_g = 2GM/c^2$ is the Schwarzschild radius. Around a protostar, this power is

$$P_{acc} \simeq 10^{32} \left(\frac{\dot{M}_{ae}}{\dot{M}_*} \right) \left(\frac{M}{.5M_\odot} \right) \left(\frac{r_i}{r_*} \right)^{-1} \text{ erg s}^{-1} \quad (13)$$

for $\dot{M}_* = 10^{-7}M_\odot \text{yr}^{-1}$, $r_* = 30r_\odot$ (10 stellar radii for a typical T-Tauri star). Since the available energy is stored into rotation, energy conservation can be rewritten as

$$\begin{aligned} 2P_{rad} &\simeq \frac{1-\Theta}{1+\Lambda} P_{lib} \\ 2P_{jet} &= \frac{\Lambda+\Theta}{1+\Lambda} P_{lib}, \end{aligned} \quad (14)$$

where $\Theta < 1$ is the fraction of the internal energy that was transferred in the jet as enthalpy. The total jet power, which can be either radiated away or injected at the terminal shock (e.g. extragalactic radio lobes), arises from the sum of the MHD Poynting flux and the plasma thermal power. Thus, magnetized accretion discs without a hot corona ($\Lambda \simeq r/h$, $\Theta = 0$) radiate only a fraction of order h/r of the jet power.

2.2. From accretion to ejection

MAES are intricate structures where accretion and ejection are interdependent. Therefore, we will frequently

make references to disc physics and quantities in our investigation of jet physics. Let us then, for the sake of completeness, summarize here results concerning magnetized disc physics.

Two simultaneous processes are responsible for accretion (FP93a): (1) a turbulent magnetic diffusivity ν_m allowing matter to steadily diffuse through the field; (2) a dominant magnetic torque $F_\phi = J_z B_r - J_r B_z$, which brakes the disc and stores into the field both angular momentum and mechanical energy of the plasma. A local quasi-magnetohydrostatic vertical equilibrium is achieved, the plasma pressure gradient hardly competing with both tidal compression and vertical magnetic pinching force. A radial magnetic tension slightly counteracts gravity, thus leading to a sub-Keplerian rotation rate.

As a result, plasma inside the disc (see Fig. 1) is being accreted, slightly converging towards the disc midplane (both u_r and u_z are negative). How then is ejection achieved?

Ejection comes out naturally if the radial current density J_r decreases vertically on a disc scale height (Ferreira & Pelletier 1993b). Indeed, in a Keplerian disc, this is the only possibility to change the sign of the magnetic torque F_ϕ . This torque must become positive at the disc surface in order to provide a magnetic acceleration. Such a situation requires that the counter current due to the disc differential rotation balances the current induced by the unipolar induction effect (FP95). If this is not fulfilled, the complete structure is unsteady: in fact, the requirement of stationarity provides the level of the “toroidal” diffusivity ν'_m .

The vertical decrease of J_r leads to the following important effects:

(1) the vertical Lorentz force decreases, allowing the plasma pressure gradient to gently lift up matter from the disc surface;

(2) matter is azimuthally accelerated by the magnetic field, leading then to a radial centrifugal acceleration. Note that, although it is plasma pressure that provides a positive vertical velocity, this process is purely magnetic. It arises naturally if the magnetic pinching force (that must be comparable to the plasma pressure gradient) decreases vertically.

In order to get an insight on the jet physical processes, it is worthwhile to project the Lorentz force parallel and perpendicular to any poloidal magnetic surface,

$$\begin{aligned} F_\phi &= \frac{B_p}{2\pi r} \nabla_{\parallel} I \\ F_{\parallel} &= -\frac{B_\phi}{2\pi r} \nabla_{\parallel} I \\ F_{\perp} &= B_p J_\phi - \frac{B_\phi}{2\pi r} \nabla_{\perp} I. \end{aligned} \quad (15)$$

Here, $I = 2\pi r B_\phi / \mu_0 < 0$ is the total current flowing within this magnetic surface, $\nabla_{\parallel} \equiv (\mathbf{B}_p \cdot \nabla) / B_p$ and $\nabla_{\perp} \equiv (\nabla a \cdot \nabla) / |\nabla a|$. This shows directly that plasma

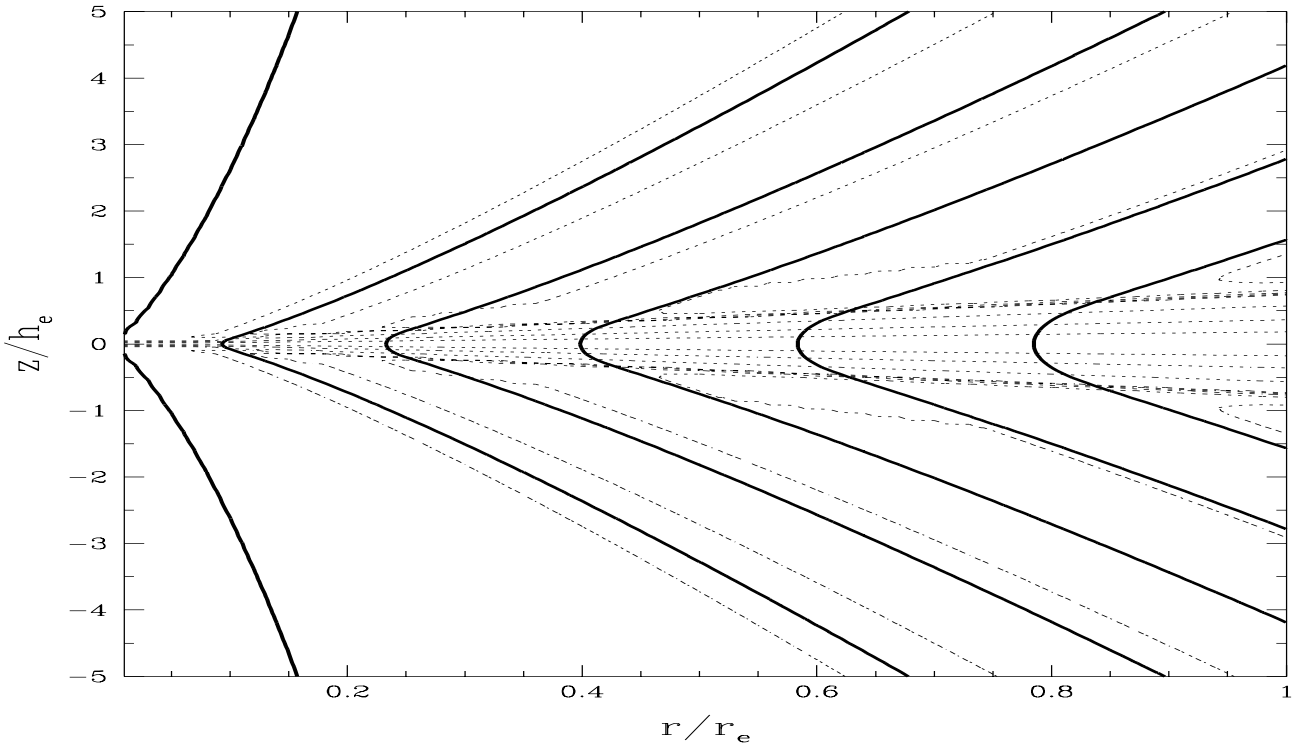


Fig. 1. Side view of a magnetized accretion disc driving jets, with $\varepsilon = 10^{-1}$, $\alpha_m = 1$ and an ejection efficiency $\xi = .004$. Plasma (dotted lines) enters the structure at its outer edge and is accreted with a slight converging motion through the magnetic field (solid lines). Since the magnetic pinching force decreases vertically, plasma reaches a layer where the pressure gradient slowly expels it. Diffusion is still necessary at the disc surface in order to allow a transition between the accretion disc and the ideal MHD jet. This transition region is approximatively one disc scale height thick. Farther out, plasma is frozen in a particular magnetic field line and is accelerated through the Lorentz force. Note the scaling factor ε^{-1} applied to the vertical axis.

is accelerated by the current leakage through this surface ($\nabla_{\parallel} I > 0$). This effect gives rise to both a poloidal (F_{\parallel}) and a toroidal (F_{ϕ}) magnetic force, the latter providing the centrifugal force. Thus, cold jets are better referred to as being magnetically-driven rather than centrifugally-driven (this was also pointed out by Contopoulos & Lovelace 1994). When the current I vanishes, or when it flows parallel to the magnetic surface, no magnetic acceleration arises anymore and the plasma reaches an asymptotic state. Note also that the way this current is distributed across the magnetic surfaces is of great importance for the jet transverse equilibrium (F_{\perp}). This shows that one has to be careful when dealing with a particular current distribution, since it is of so great importance in both jet collimation and acceleration (Appl & Camenzind 1993a, 1993b).

The global current topology is linked to the ejection efficiency, which is measured by the ejection index ξ ($\xi = 0$ in a viscous disc without jet). For small ejection efficiencies ($\xi < 1/2$), ejection takes place against a pinching vertical Lorentz force, with a positive radial component. For those tenuous ejections, the current enters the disc at its inner edge, flows up inside the jet and closes back

along the axis. High ejection efficiencies ($\xi > 1/2$) are achieved when matter is lifted by both plasma and magnetic pressure gradients (positive vertical Lorentz force), the corresponding radial Lorentz force being negative. In this case, the current flows down the jet, enters the disc at its surface and closes in an outer cocoon (Ferreira 1994).

The set of MAES parameters (8) is diminished by the requirement that the overall structure is in steady-state. This implies that the flow has to smoothly cross the usual MHD critical points it encounters (see FP95). The constraint due to the first critical point, the slow-magnetosonic (SM) point, allows these two current topologies to be realized. In what follows, we will show that only tenuous ejections can produce trans-Alfvénic jets.

3. Non-relativistic, magnetically-driven jets from Keplerian discs

3.1. Governing equations

Above the disc, both the decay of the turbulent diffusivity and the action of the poloidal Lorentz force leads matter into ideal MHD state (Ferreira 1996). In this state,

matter is frozen in the field, the poloidal motion occurring along a magnetic surface. Together with axisymmetry, this allows to describe jets as a bunch of magnetic surfaces, nested on the accretion disc at an anchoring radius r_o . In this section, we write the well-known governing equations for self-confined jets in a form similar to the one Pelletier & Pudritz (1992, hereafter PP92) used. Written in such a form, these equations will allow us to derive general properties and conditions for non-relativistic, magnetically-driven jets when one takes into account the underlying disc. In Sect. 4, we will come back to the set of equations as described in Sect. 2 and solve them from the disc equatorial plane to the “jet end”.

In the ideal MHD jet, Eq.(4) becomes

$$\mathbf{u}_p = \frac{\eta(a)}{\mu_o \rho} \mathbf{B}_p, \quad (16)$$

where $\eta(a)$ is a constant along a particular magnetic surface. Its value, $\eta = \sqrt{\mu_o \rho_A}$, is directly evaluated at the Alfvén point (labelled with the cylindrical coordinates r_A and z_A), where the jet poloidal velocity reaches the local Alfvén speed. Equation (5) becomes

$$\Omega_*(a) = \Omega - \eta \frac{B_\phi}{\mu_o \rho r}, \quad (17)$$

and defines the rotation rate Ω_* of a magnetic surface. Since the field lines are anchored on the accretion disc, they rotate with roughly the same rotation rate as matter, namely $\Omega_* \simeq \Omega_o$. Thus, one can look at this equation as providing the amount of toroidal field required to maintain matter, which is frozen in the field, rotating in the jet at a different rate than the field.

Using these two equations, the steady-state angular momentum conservation equation can then be written as

$$\Omega_* r_A^2 = \Omega r^2 - \frac{r B_\phi}{\eta} \quad (18)$$

where $\Omega_* r_A^2$ is the total specific angular momentum carried away by both matter and field in a particular magnetic surface. The radial and vertical momentum conservation equations are usually replaced by their projection along (Bernoulli equation) and perpendicular (Grad-Shafranov equation, also known as transfield equation, Tsinganos 1981) to such a magnetic surface. For polytropic flows, Bernoulli equation reads

$$\frac{u^2}{2} + H + \phi_G - \Omega_* \frac{r B_\phi}{\eta} = E(a) \quad (19)$$

where $E(a)$ is the constant specific energy carried by the jet and the jet enthalpy H is defined as $\nabla H = \nabla P/\rho$. For magnetically-driven jets (i.e. cold), this enthalpy plays no role neither in jet formation nor in its collimation. Indeed, it is only a fraction of order ε^2 of the Keplerian speed and so it will be simply dropped in the following section

(but note that the solutions in Sect. 4 are obtained with the full set of self-similar MHD equations). As shown in FP95, ejection of matter from the disc arises naturally due to the vertical decrease, on a disc scale height, of the radial current density. This is a pure magnetic process, without any help from thermal effects. On the contrary, thermally-driven jets require a high enthalpy with a polytropic index γ variable along a magnetic surface, namely close to unity near the disc to account for coronal heating and closer to the adiabatic value further away (Weber & Davis 1967, Tsinganos & Trussoni 1991, Sauty & Tsinganos 1994). This last possibility is postponed to future work. Bernoulli equation (19) describes how the total energy carried by the flow is transformed into kinetic energy, for a given magnetic configuration. Hence, one can interpret this equation as providing the velocity matter reaches in a given “magnetic funnel”. The shape of this funnel, or more precisely the jet transverse equilibrium, is provided by Grad-Shafranov equation

$$\nabla \cdot (m^2 - 1) \frac{\nabla a}{\mu_o r^2} = \rho \left\{ \frac{dE}{da} - \Omega \frac{d\Omega_* r_A^2}{da} \right. \\ \left. + (\Omega r^2 - \Omega_* r_A^2) \frac{d\Omega_*}{da} \right\} \\ + \frac{B_\phi^2 + m^2 B_p^2}{2\mu_o} \frac{d \ln \rho_A}{da} \quad (20)$$

where we introduced the Alfvénic Mach number $m^2 \equiv u_p^2/V_{Ap}^2$.

The set of equations (16) to (20), together with Eq.(7), completely describe magnetic jets where plasma pressure plays no dynamical role. Hereafter, we describe the leading parameters of these equations.

3.2. An unique parameter for cold jets

We choose to characterize our jet solutions by using parameters as defined in the pioneering work of BP82. Since each parameter is strictly defined at the footpoint r_o of a magnetic surface, it characterizes the jet state only locally. Thus, in a realistic 2-D case, one would have to prescribe them for a range of anchoring radii in the disc. However, if we assume that jets are produced from a large radial extension in the disc, then we can look for a jet solution defined with parameters that are constants (as in self-similar solutions), or slowly varying with the radius. Through all this paper, we will label with a subscript “o” any quantity evaluated at the disc midplane and a subscript “A” at the Alfvén surface. In particular, $\rho_o = \rho(r_o, 0)$ will be the midplane density and $u_o = -u_r(r_o, 0)$ the accretion velocity at a radius r_o .

The first parameter describes the magnetic configuration, namely

$$\beta \equiv \frac{d \ln a}{d \ln r_o} \quad (21)$$

with $0 < \beta < 2$ (FP93a). Jets with constant β have a magnetic field varying with a power law of the radius. BP82's self-similar solutions were obtained with the prescription $\beta = 3/4$. The second parameter, defined as

$$\lambda \equiv \frac{\Omega_* r_A^2}{\Omega_o r_o^2} \simeq \frac{r_A^2}{r_o^2} \quad (22)$$

is a measure of the magnetic lever arm that brakes the underlying accretion disc. Since the available energy is stored in the disc as rotational energy, a constraint on this lever arm arises through the requirement that jets are powered with a positive energy. Indeed, the total specific energy carried away by the (cold) magnetic structure writes

$$E(a) = \mathcal{E}(a) + \Omega_*^2 r_A^2 \quad (23)$$

where $\mathcal{E}(a) \simeq -3\Omega_o^2 r_o^2/2$. Jets become free from the potential well if the "rotator" energy, namely $\Omega_*^2 r_A^2$, overcomes the generalized pressure \mathcal{E} (PP92). This is fulfilled provided $\lambda > 3/2$. The last parameter,

$$\kappa \equiv \eta \frac{\Omega_o r_o}{B_o} \quad (24)$$

measures the mass load on a particular magnetic surface. Since cold jets carry away the whole disc angular momentum, one expects to find a systematic relation between mass load and lever arm.

These parameters must be linked to the ejection index, since it is a local measure of the ejection efficiency. A way to find such a link is to look at the ratio of the MHD Poynting flux to the kinetic energy flux along a magnetic surface,

$$\sigma = \frac{-2\Omega_* r B_\phi B_p}{\mu_o \rho u^2 u_p} \quad (25)$$

Such a ratio measures the amount of energy stored as magnetic energy with respect to the kinetic energy, being therefore a measure along the jet of the acceleration efficiency. At the jet basis, identified here as the SM-surface, the disc provides

$$\sigma_{SM} = \frac{\dot{M}_a}{2\pi\rho u_z r_o^2} \frac{-B_\phi B_z}{\mu_o \rho_o u_o \Omega_o h} \simeq \xi^{-1} \quad (26)$$

where we used mass ($d\dot{M}_a/dr = 2d\dot{M}_j/dr = 4\pi\rho u_z r$) and angular momentum conservation. Thus, the ejection index is also quite accurately the injection of energy into the jets. While the magnetic lever arm is directly $\lambda = 1 + \sigma_{SM}/2$, the mass load writes

$$\kappa = 2\sigma_{SM}^{-1} \left| \frac{B_{\phi,SM}}{B_o} \right|, \quad (27)$$

which provides $\kappa \simeq q\xi \sim \xi$ (see Appendix B). Thus, the leading parameters for magnetically-driven jets can

be simply expressed as

$$\begin{aligned} \beta &= \frac{3}{4} + \frac{\xi}{2} \\ \lambda &\simeq 1 + \frac{1}{2\xi} \\ \kappa &\simeq \xi \end{aligned} \quad (28)$$

The expression for the magnetic configuration parameter β is general for any Keplerian disc, allowing to take into account simultaneously magnetic and gravitational terms (FP93a, FP95). All three parameters for cold jets can be quite accurately replaced by ξ : magnetic configuration and both mass load and lever arm are therefore tightly related. As a consequence, the parameter space for cold jets is mostly controlled by the range of allowed ejection indices.

By using (28), we are now able to see that any jet model that would allow ejection with a high efficiency (namely, $\xi \geq 1$) would not obtain free jets ($E(a) \leq 0$). Nevertheless, jet solutions that successfully cross the SM-point with $\xi > 1$ were found to be possible (Ferreira 1994). Such a situation is therefore a transient feature, matter failing to reach the Alfvén surface and falling down to the disc after having been ejected out.

3.3. Constraints on the ejection index

3.3.1. Minimum ejection index: disc vertical equilibrium

A look at the parameter space in FP95, derived with the sole constraint due to the slow-magnetosonic point, indicates that there is a minimum ejection index ξ_{min} . Here, we show that this minimum ejection efficiency is related to the existence of a quasi-magnetohydrostatic (MHS) equilibrium inside the disc. Such an equilibrium, described by

$$\rho u_z \frac{\partial u_z}{\partial z} \simeq -\frac{\partial P}{\partial z} - \rho \Omega_K^2 z - \frac{\partial}{\partial z} \frac{B_r^2 + B_\phi^2}{2\mu_o}, \quad (29)$$

is obtained when plasma pressure gradient balances both tidal compression and magnetic squeezing. This magnetic squeezing depends on the value of the magnetic field, measured by the parameter μ (see Eq.(8)), and on both curvature (for B_r) and shear (for B_ϕ) effects. When the ejection efficiency decreases, the lever arm increases and so does the magnetic compression due to field curvature. The only way to find out another equilibrium state is then to decrease the value of the field itself (that is, μ). However, this results in an enhancement of the magnetic squeezing due to shear.

This can be qualitatively shown like follows (for more details, see Appendices B and C). The induction equation (5) can be written in the disc as

$$\eta'_m J_r \simeq \eta'_o J_o + r \int_0^z dz \mathbf{B}_p \cdot \nabla \Omega - B_\phi u_z \quad (30)$$

where the last term describes the effect of advection. In the resistive disc, this term is negligible in comparison with the others. Thus, the toroidal field at the disc surface,

$$B_\phi^+ = B_\phi^{J_o} + B_\phi^{\nabla\Omega} \quad (31)$$

is mainly the sum of two contributions, $B_\phi^{J_o} = -\mu_o J_o h$ due to the unipolar induction effect and $B_\phi^{\nabla\Omega}$, the counter current (of positive sign) provided by the disc differential rotation. If the disc were rigidly rotating (i.e., a Barlow Wheel), it would generate the first contribution but not the second one, therefore producing no jet. When μ decreases, the magnitude of this counter current decreases, thereby increasing the toroidal field at the disc surface and with it, the pinching effect of the corresponding magnetic pressure gradient.

There is thus a ξ_{min} below which no quasi-MHS equilibrium can be found anymore. The exact value of this minimum ejection index is impossible to find analytically, since it depends on a subtle equilibrium between terms that are all of the same order of magnitude. When such equilibrium is crudely treated, one can in principle still obtain a matching with jet solutions but the disc would certainly not survive an overwhelming magnetic squeezing.

In Section 4, we show the parameter space obtained for self-similar solutions, thus providing a numerical value for ξ_{min} . Because self-similarity does not influence solutions close to the Keplerian disc but allows instead to take into account all dynamical terms, we believe that this value is general. Since what limits the minimum ejection index is the increasing toroidal field, one can only significantly lower ξ_{min} by decreasing the value of $B_\phi^{J_o}$, that is, by lowering J_o . Therefore, only discs where both viscosity and magnetic torques are relevant ($\Lambda \lesssim 1$, requiring a hot corona to produce jets), should allow ejection indices much smaller than those displayed here.

3.3.2. Maximum ejection index: jet acceleration

Conservation of angular momentum (Eq.(18)) implies that once a large scale magnetic field steadily brakes the disc with a significant torque, matter must be accelerated up to the Alfvén point. This severely constrains the mass load in the jet, thus providing an upper limit on the ejection index. When gravity becomes negligible, Bernoulli equation can be rewritten (FP93a) as

$$\alpha^2 \equiv \frac{u_p^2}{\Omega_o^2 r_o^2} = (1 - g^2) \frac{r^2}{r_o^2} - 3 \quad (32)$$

where the function g , defined as $\Omega = \Omega_*(1 - g)$, can be expressed as

$$g = \frac{m^2}{m^2 - 1} \left(1 - \frac{r_A^2}{r^2} \right) . \quad (33)$$

It measures the discrepancy between the angular velocities of matter and magnetic surface on which matter flows (PP92). At the jet basis, its value is approximately zero, then it increases and reaches unity for highly super-Alfvénic jets. The Alfvénic Mach number becomes then simply

$$m^2 = \alpha \kappa \frac{B_o}{B_p} . \quad (34)$$

A necessary condition for trans-Alfvénic jets is obtained by requiring that the above expression reaches or becomes much bigger than unity. At this stage, it is convenient to introduce the ratio, measured at the Alfvén point, of the rotation velocity of the magnetic surface to the poloidal Alfvén speed (Michel 1969, PP92)

$$\omega_A \equiv \frac{\Omega_* r_A}{V_{Ap,A}} = \kappa \lambda^{1/2} \frac{B_o}{B_{p,A}} . \quad (35)$$

This fastness parameter is a useful quantity since it encloses an information that we cannot have without solving first the whole structure, namely the angle of the poloidal magnetic field with respect to the vertical axis. This ratio, which must verify

$$\omega_A > \left| \frac{B_\phi}{B_p} \right|_A , \quad (36)$$

will allow us to derive a general condition for trans-Alfvénic jets, in two extreme cases.

For “powerful” jets (high σ_{SM}), matter is expelled off the disc carrying almost no angular momentum. Acceleration takes place only if $\sigma_A < \sigma_{SM}$, with $\sigma_A \simeq 2\omega_A^2$. Thus, these jets require

$$\omega_A^2 < \frac{1}{2\xi} . \quad (37)$$

This corresponds to the extreme case where it takes almost no power from the magnetic structure to accelerate plasma up to the Alfvén surface. Such a configuration could be obtained in the low mass load limit.

For “weak” jets (low σ_{SM}), the Alfvénic Mach number has to reach at least unity. At the Alfvén point, Bernoulli equation writes $\alpha_A^2 = (1 - g_A^2) \lambda - 3$. This shows that matter reaches its maximum velocity when $g_A = 0$, namely when the toroidal field is almost zero. Using Eq.(34), it can be seen that these jets require

$$\omega_A^2 = \frac{\lambda}{\alpha_A^2} > \frac{\lambda}{\lambda - 3} . \quad (38)$$

This general condition shows that magnetically-driven jets are fast rotators ($\omega_A > 1$) in order to successfully reach the Alfvén surface (BP82, PP92, Rosso & Pelletier 1994). This is required even in this case, where matter barely reaches it despite the almost complete transfer of energy

from the magnetic structure. High mass loads could give rise to such jets.

Compiling criteria (37) and (38), one gets the necessary condition for trans-Alfvénic jets

$$\frac{1+2\xi}{1-4\xi} < \omega_A^2 < \frac{1}{2\xi}, \quad (39)$$

which must be satisfied at each magnetic surface. Here, we get a much more precise constraint since it requires

$$\xi < \frac{\sqrt{13}-3}{4} \simeq 0.15. \quad (40)$$

This implies that higher ejection efficiencies are completely inconsistent with a steady trans-Alfvénic regime. Note that this value should be viewed as an upper limit for ξ , the maximum ejection index ξ_{max} being in fact smaller. This is due to the weak constraint we used in the high- σ_{SM} case. Contopoulos (1995) proposed a simple jet model where the magnetic field has only a toroidal component. In such a case (obtained in the limit κ very large), the Alfvén singularity disappears and the driving mechanism for jet acceleration is the magnetic pressure gradient. We would like to stress that such a configuration is, in principle, possible as a transient outburst from thin discs. Indeed, FP95 showed that magnetically-driven jets can be viewed as being either “centrifugally-driven” for small ejection indices ($\xi < 1/2$, the vertical component of the Lorentz force pinching the disc) or “magnetic pressure-driven” for high ejection indices ($\xi > 1/2$, the toroidal magnetic pressure lifting matter up, consistent with the large κ limit used). However, only the first situation allows a steady state with respect to the Alfvén surface. The possibility remains that such a configuration would be steadily produced by a thick disc. In the next section, we compute global self-similar solutions, derive both ξ_{min} and ξ_{max} numerically and obtain the full parameter space for cold MAES.

4. Trans-Alfvénic, global disc-jet solutions

4.1. The self-similar ansatz

In order to construct global solutions from the disc equatorial plane up to a jet asymptotic regime, the full set of non-linear, partial differential equations (1) to (5) along with Eq.(7) must be solved. Since MAES are intrinsically 2-D, this requires either a numerical approach (not yet available) or some method to reduce this set to a set of ordinary differential equations (but enforcing some symmetry to solutions). This is what allows self-similarity, which is the reason why it has been used by many authors (see Tsinganos et al. (1996) for a review).

We look then for self-similar solutions so that any quantity Q can be written

$$Q(r, z) = Q_e \left(\frac{r}{r_e} \right)^{\alpha_Q} f_Q(x), \quad (41)$$

where r_e is the external radius of the disc (a standard viscous disc is probably established from r_e to larger radii). The self-similar variable is chosen to be $x \equiv z/h(r)$, consistent with the gravity field at the disc neighbourhood, but also everywhere since $h(r) = \varepsilon r$. Such a form, $h \propto r$, is expected to arise in a Keplerian disc pervaded by a large scale magnetic field (FP93a, FP95). The magnetic flux function is chosen to be

$$a(r, z) = a_e \left(\frac{r}{r_e} \right)^\beta \psi(x) \quad (42)$$

where $\psi(-x) = \psi(x)$ and the pressure prescription such that $\mathcal{K}(a) = \mathcal{K}_e(r_o/r_e)^{\alpha_K}$, with $\alpha_K = (1-\gamma)(2\beta-3)-1$, the polytropic index γ remaining a free parameter. Since we focus on cold jets, its value has no importance and we choose $\gamma = 1$ for convenience (see discussion after Eq.(7)).

The set of PDEs can be separated into two sets, the first consisting of algebraic equations between the indices α_Q and β , the second of non-linear ODEs on the functions f_Q , ψ and their derivatives (see Appendix B in FP95). Within such a prescription, all the dynamical terms can be included, allowing henceforth a complete study of the physics of ejection from Keplerian discs. However, only non-relativistic jets can be studied within the same self-similarity prescription. Indeed, relativistic speeds enforce a scaling with the speed of light (Li et al. 1992), which is inconsistent with disc physics.

Since the boundary values $f_Q(0)$ at the disc midplane are known, we just have to integrate the set of ODEs from $x = 0$ to infinity. Once we have a global solution as a function of $x = z/\varepsilon r$, it is straightforward to obtain the variation of any quantity along any magnetic surface $a = constant$ with

$$Q(x(a)) = Q_o f(x) \psi(x)^{-\alpha_Q/\beta} \quad (43)$$

where $Q_o = Q_e(r_o/r_e)^{\alpha_Q}$ (note the use of the notation $x(a)$ in this case). The main difficulties come from the presence of three critical points, whenever the plasma velocity $V \equiv \mathbf{u} \cdot \mathbf{n}$, where

$$\mathbf{n} \equiv \frac{\mathbf{e}_z - \varepsilon x \mathbf{e}_r}{\sqrt{1 + \varepsilon^2 x^2}}, \quad (44)$$

equals the three usual MHD phase speeds: slow-magnetosonic, Alfvén and fast-magnetosonic, in the direction \mathbf{n} . Self-similarity not only modifies the definitions of these phase speeds, but constrains also the direction of propagation where critical points appear (see FP95 for more precisions). Hence, the critical velocity V is roughly u_z at the disc neighbourhood where the flow becomes super-SM, and u_r much farther away.

4.2. MAES parameter space

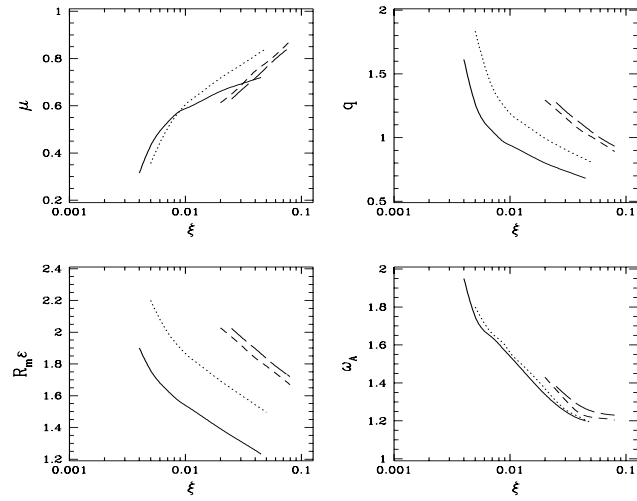


Fig. 2. MAES parameter space for an isothermal structure with $\alpha_m = 1$, for various disc aspect ratios: $\varepsilon = 10^{-1}$ (solid line), 10^{-2} (dotted line), 10^{-3} (short-dashed line) and $7 \cdot 10^{-4}$ (long-dashed line). The disc magnetization μ and the magnetic Reynolds number \mathcal{R}_m were obtained as regularity conditions, in order to get respectively trans-SM and trans-Alfvénic solutions. The other two parameters, the magnetic shear at the disc surface q and fastness parameter ω_A are calculated. As ξ decreases, μ must decrease in order to balance the increase in magnetic shear q and curvature $\mathcal{R}_m \varepsilon$ (see Sect. 3.3.1). It is noteworthy that, although the disc parameters change a little, the main effect of decreasing ε is to shift the range of allowed ξ to higher values. We confirm here that trans-Alfvénic jets require $\omega_A \gtrsim 1$ (PP92, Rosso & Pelletier 1994).

4.2.1. The slow-magnetosonic point

We obtain trans-SM solutions by adjusting the strength of the field for a given set of parameters (FP95). Thus, for μ bigger than a critical value μ_c , the magnetic compression is too strong and leads to a vanishing density (hence infinite vertical acceleration). When $\mu < \mu_c$, the magnetic compression is insufficient and too much mass is expelled off, which eventually falls down again.

Thus, the smooth crossing of the first critical point is directly related to the disc vertical balance. Following Li (1995), we can express that a necessary (but not sufficient) condition for stationarity is

$$P_o \gtrsim \frac{B_r^2 + B_\phi^2}{2\mu_o} \Big|_+ \quad (45)$$

where the subscript “+” refers to the disc surface. In terms of MAES parameters, this condition for cold jets becomes

$$\mu \lesssim \frac{8 - \alpha_m^2 \mathcal{R}_m^2 \varepsilon^2 f_+^2}{4\mathcal{R}_m^2 \varepsilon^2} \quad (46)$$

where the function f_+ is of order unity (see Appendix B). This implies $\mu < 3/2$, which shows that jets cannot be produced from magnetically dominated discs. Since plasma pressure plays such an important role in sustaining the disc, only structures close to equipartition are steady (FP95).

The minimum ejection index ξ_{min} is found by requiring that all solutions become super-SM. We found $\xi_{min} = 0.004$ for an isothermal disc with $\varepsilon = 0.1$ and $\alpha_m = 1$. If the disc aspect ratio ε (and also the turbulence level α_m , see below) decreases, the influence of advection in Eq.(30) also decreases and the radial current density J_r is smaller, hence providing a smaller value of the toroidal field at the disc surface (f_+ , see Appendix C). As an example, we obtain $f_+ \simeq 0.6, 0.5, 0.45$ for $\varepsilon = 0.1, 0.01, 0.001$ respectively. The magnetic compression decreasing, the range of allowed ejection efficiencies is shifted to higher values (see Fig. 2). Moreover, by using an isothermal prescription for the disc temperature, we have underestimated the “lifting” efficiency of the plasma pressure gradient. Thus, $\xi_{min} = 0.004$ should be seen as the lower limit for cold jets from Keplerian discs. However, since $\xi < 0.15$ is a general constraint, one can expect to find that below a certain value of ε (and α_m), no steady-state solutions can be found anymore.

The work presented here strongly differs from the work done by Wardle & Königl (1993) and Li (1995). These authors found no limiting ξ and were thus able to obtain jet solutions with an enormous lever arm λ , and an arbitrarily small mass load κ . Here, it has been found that such a situation is impossible to achieve in steady-state. This disagreement comes from their different treatment of the highly sensitive disc vertical equilibrium. Indeed, Wardle & Königl investigated the vertical structure at a given radius and made the assumption (valid for the jet) $\rho u_z = \text{constant}$ in order to deal with the mass conservation equation. Li used a self-similar approach, but did not make a smooth transition between the disc and its jets, crudely matching the disc MHS solutions to jet ones. He however found that the mass load was very sensitive to the plasma rotation rate at the disc midplane Ω_o : the smaller Ω_o the smaller κ . This can now be understood with what was previously said. Indeed, $\Omega_o = \Omega_k(1 - \omega_o)$ with $\omega_o \simeq \mu \mathcal{R}_m \varepsilon^2 / 2 = o(\varepsilon)$. Thus, a smaller Ω_o is achieved with a bigger ε , which implies a smaller ejection efficiency (hence, $\kappa \simeq \xi$).

4.2.2. The Alfvén point

In order to get trans-Alfvénic solutions, we adjust the magnetic Reynolds number \mathcal{R}_m , which controls the bending of the poloidal field lines at the disc surface. For \mathcal{R}_m bigger than a critical value \mathcal{R}_c , the bending is too strong and leads to an overwhelming centrifugal effect, such that $\Omega r^2 > \Omega_* r_A^2$ (i.e., B_ϕ becomes unphysically positive). On the contrary, if $\mathcal{R}_m < \mathcal{R}_c$, the centrifugal effect cannot bal-

ance the magnetic tension, which leads to an unphysical closure of the magnetic surfaces (B_r becomes negative). At each trial for \mathcal{R}_m one has to find another critical μ_c that allows a super-SM solution. Note that fixing \mathcal{R}_m is the same as fixing the accretion velocity at the disc midplane, for any given magnetic diffusivity. We have the freedom to do it because this accretion velocity is also controlled by the magnetic field. If we were in a situation where accretion is mainly due to the viscous stress, then \mathcal{R}_m would also be given.

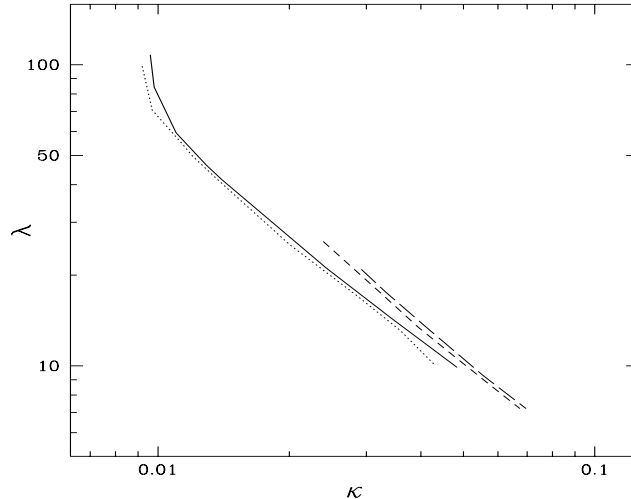


Fig. 3. Parameter space for cold jets launched from an isothermal accretion disc, with $\alpha_m = 1$ and for various disc aspect ratios: $\varepsilon = 10^{-1}$ (solid line), 10^{-2} (dotted line), 10^{-3} (short-dashed line) and $7 10^{-4}$ (long-dashed line). Due to the SM constraint, we get here a smaller parameter space as in BP82. As showed, the jet parameters do not significantly vary with any parameter but ξ .

Figure 3 shows the parameter space for cold jets in the κ - Λ plane for $\alpha_m = 1$. Solutions with $\kappa > 0.1$ do not allow super-Alfvénic jets (BP82, Wardle & Königl 1993). We found here that $\xi_{max} = .08$, the maximum Alfvénic Mach number reached by the flow being barely bigger than unity. For disc aspect ratios below $5 10^{-4}$, no steady-state solutions are found, ξ_{min} becoming equal to ξ_{max} . Thus, trans-Alfvénic jets are produced for discs where $5 10^{-4} < \varepsilon \leq 10^{-1}$, the upper bound arising from the thin-disc approximation.

Using Eq.(16), we can express the density at the Alfvén point as a function of the disc midplane density and MAES parameters, namely

$$\frac{\rho_A}{\rho_o} \simeq \frac{\alpha_m^2}{4} \mathcal{R}_m^2 \varepsilon^4 \xi^2. \quad (47)$$

This relation is local and independent of any boundary condition that could constrain the jet behaviour. Since

we approximately obtain numerically such a value for the Alfvén density, as well as a consistency with all our general requirements of Sect. 3.3.2, we believe that self-similarity doesn't affect the solutions up to this point. Therefore, our parameter space should be viewed as general for cold jets launched from Keplerian discs.

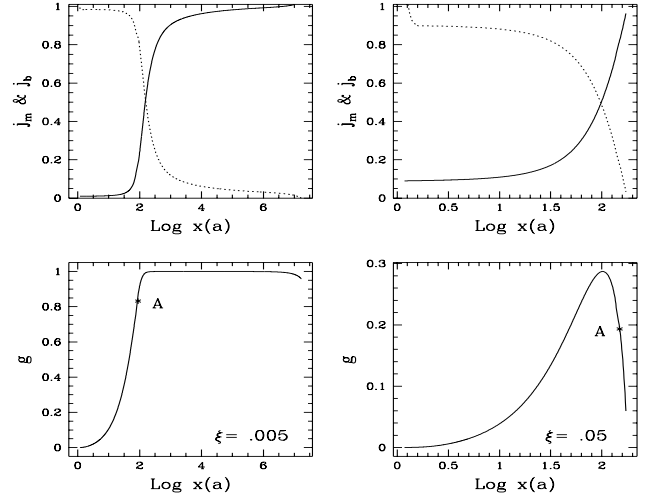


Fig. 4. Low-efficiency ($\xi = 0.005$, left panels) and high-efficiency ($\xi = 0.05$, right panels) trans-Alfvénic jets for $\varepsilon = 10^{-2}$, $\alpha_m = 1$. The upper panels show the angular momentum transfer from the field (j_b , dashed line), to the plasma (j_m , solid line). At the disc surface ($x = 1$), all the specific angular momentum $\Omega_* r_A^2$ is carried by the field, but it is afterwards completely transferred into the plasma. Below, the corresponding function $g = 1 - \Omega/\Omega_*$ is displayed for both cases. The cross labelled with “A” tells the position of the Alfvén surface. In the low-efficiency limit, the jet reaches it with $g \sim 1$ ($\omega_A = 1.8$), most of the power being still carried by the field. In the high-efficiency case, the flow requires already almost all the power to reach Alfvén speeds ($\omega_A = 1.19$).

At this stage, one cannot tell with precision what will be the asymptotic state of the jet (unless of course by propagating the solution, as we will do next section). However, by using general arguments based on the work of Heyvaerts & Norman (1989), one can give clues on the degree of collimation achieved, according to the amount of current I_A

$$\frac{I_A}{I_{SM}} = g_A (1 + 2\sigma_{SM}^{-1}) \simeq g_A \quad (48)$$

still available at the Alfvén point. Hereafter, we make a distinction between two kinds of jets, depending upon their state at the Alfvén surface (see Fig. 4).

Current-carrying jets ($g_A \lesssim 1$) reach the Alfvén surface while most of the angular momentum is still stored in the magnetic structure. They are powerful (corresponding here to “low” ejection indices $0.004 \leq \xi \lesssim 0.025$) and

could reach highly super-Alfvénic speeds ($m^2 \gg 1$), with $\Omega \simeq \Omega_* r_A^2 / r^2$ and a maximum poloidal velocity

$$u_{p,max} = \Omega_o r_o (2\lambda - 3)^{1/2}. \quad (49)$$

Such jets could allow a cylindrical collimation if this current does not vanish completely.

Current-free jets ($g_A \ll 1$) become super-Alfvénic at the expense of almost all the available current. They correspond to “high” ejection efficiencies $0.025 \lesssim \xi \leq 0.08$ (for $\alpha_m = 1$, see below). According to Heyvaerts & Norman, only parabolic collimation could be asymptotically achieved. These jets could reach moderate speeds ($m^2 \geq 1$), with $\Omega \lesssim \Omega_*$ and a maximum poloidal velocity

$$u_{p,max} = \Omega_o r_o (\lambda - 3)^{1/2}. \quad (50)$$

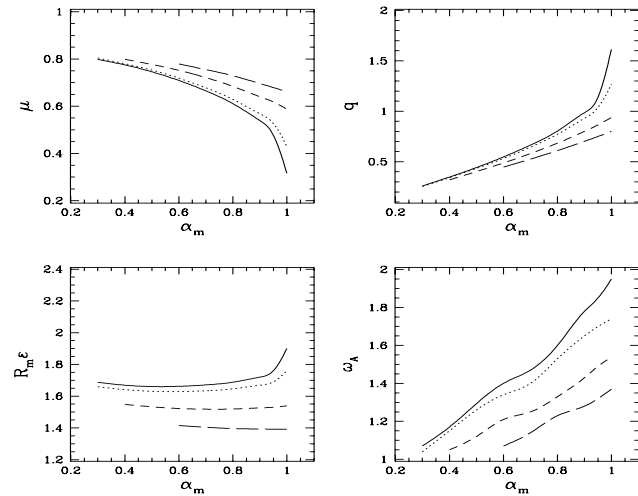


Fig. 5. Influence of the turbulence parameter α_m on other MAES parameters (see Fig. 2), for $\varepsilon = 10^{-1}$ and various ejection indices: $\xi = 0.004$ (solid line), 0.005 (dotted line), 0.01 (short-dashed line) and 0.02 (long-dashed line). The minimum level of MHD turbulence is limited by the value of the induced toroidal field that allows trans-Alfvénic jets ($\omega_A > 1$). The maximum level is arbitrarily fixed to unity. Note that for fixed α_m , the fastness parameter ω_A grows with decreasing ξ (see text).

4.2.3. Influence of the magnetic diffusivity

In the above two sections, we restricted ourselves to discs with $\alpha_m = 1$. Figure 5 shows that it has a profound effect on the fastness parameter ω_A : at constant ξ , the smaller α_m the smaller ω_A . Since trans-Alfvénic jets require $\omega_A > 1$, we obtain that there is a minimum turbulence level required. Because usual dimensional arguments restrict α_m to unity, we conclude that steady state MAES require an MHD turbulence with $0.1 < \alpha_m \lesssim 1$.

Equation (35) provides, for small ejection indices (Pelletier et al. 1996),

$$\omega_A \gtrsim \frac{q}{4} \xi^{-1/2} = \frac{\alpha_m}{8} \mathcal{R}_m \varepsilon \mu^{-1/2} \xi^{-1/2}. \quad (51)$$

The fastness parameter ω_A strongly depends on both the shear parameter q (henceforth on α_m) and the ejection index ξ . The highest value of ω_A (hence, of g_A) will be achieved with $\alpha_m = 1$ and the smallest value of ξ . Since the disc vertical equilibrium limits the latter, ω_A is therefore also limited ($1 < \omega_A < 2$, see Figs. 3 and 5).

As α_m decreases, the influence of plasma on the field grows: the counter current due to the disc differential rotation increases, as well as the effect of advection (see Appendix C). Thus, the toroidal magnetic field at the disc surface decreases, decreasing accordingly the magnetic torque. This has two consequences. First, the mass load is slightly lowered (see Eq.(47)), providing a higher Alfvén speed at the Alfvén surface and a lower fastness parameter. Second, the jet is less powerful (σ_{SM} decreases) and the magnetic force (F_\perp , see Eq.(15)) is less efficient in opening the jet: r_A/r_o decreases while z_A/r_o increases. In order to accelerate plasma up to the Alfvén surface, the magnetic structure has to provide more power (through F_ϕ and F_\parallel), thereby reducing the available current flowing inside a given magnetic surface (g_A decreases). Therefore, powerful jets with current still available at the Alfvén surface require a high diffusivity level ($\alpha_m \sim 1$).

We can now generalize our understanding of the asymptotic behaviour of super-Alfvénic jets by using ω_A instead of ξ . Indeed, although the jet parameters are mostly described by ξ , the jet asymptotic behaviour is drastically sensitive to ω_A .

5. Asymptotic behaviour of self-similar jets

5.1. The fate of self-similar, non-relativistic jets

When integrated up to “infinity”, all our solutions display the same behaviour: after an initial widening, the magnetic surfaces reach a maximum radius r_t and then start to bend towards the jet axis (see Figs. 6 and 7). The acceleration efficiency is very high, since the magnetic structure converts almost all the MHD Poynting flux into kinetic power ($\sigma \ll 1$), allowing therefore matter to reach its maximum velocity (see Figs. 8 and 9). They finally stop at a finite distance, with a cylindrical radius larger than the Alfvén radius r_A (Figs. 6 and 7). We are then faced to the following obvious questions: Why do our solutions stop ? and why do they always recollimate ?

The refocusing of the magnetic surfaces towards the jet axis stops because the flow meets the fast-magnetosonic (FM) critical point (see Fig. 10). The associated Mach number is defined as $t^2 = V^2 / V_{FM}^2$, where $V \simeq u_r$ at those

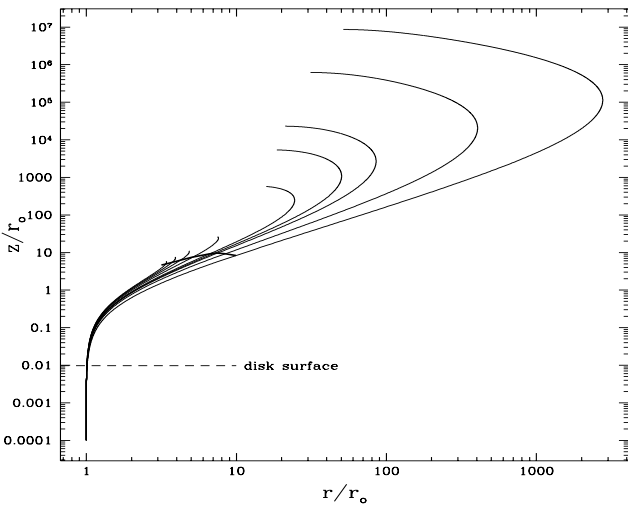


Fig. 6. Poloidal magnetic field lines for $\varepsilon = 10^{-2}$ and $\alpha_m = 1$, for $\xi = 0.05, 0.04, 0.03, 0.02, 0.012, 0.01, 0.009, 0.007$ and 0.005 (the maximum radius increases with decreasing ejection index). The thick line connects the position of the Alfvén point for each solution. Note that in the range of allowed ejection indices for $\alpha_m = 1$, the appearance of jets remains quite variable: for an anchoring radius $r_o = 10^{-1}$ AU from a young star, jets can propagate from 1 to 10^6 AU of the central source, with a maximum radius ranging from 1 to approximately 300 AU. Note the logarithmic scales: small ξ jets recollimate with angles smaller than one degree (Fig. 7).

altitudes (FP95). In the limit of super-Alfvénic speeds ($g \simeq 1$), this Mach number can be written as

$$t^2 \simeq \omega_A \left(\frac{2\lambda - 3}{\lambda} \right)^{1/2} \frac{r^2}{r_A^2} \sin^2 \theta \quad (52)$$

where θ is the jet opening angle (Fig. 7). In the other extreme limit ($g \simeq 0$), one has $t^2 \simeq m^2 \sin^2 \theta$. Thus, as the jet refocuses towards the axis (but with $r > r_A$), its opening angle grows and $t^2 = 1$ is unavoidable.

The integration scheme stopped because no regularity condition was imposed. A priori, such a critical point could (and should) be smoothly crossed if, inside our parameter range, we could obtain two characteristic behaviours at its vicinity. But we never obtained “breeze”-like solutions, all of them ending like in Fig. 10, in a way very similar to Fendt et al. (1995). Since we believe that our parameter space is weakly affected by the self-similar ansatz used, it seems to us doubtful that any physical trans-FM solution could be found. One should bear in mind that, to this date, there is no semi-analytical jet solution propagating to infinity that crosses all three critical points (slow, Alfvén and fast). Providing a precise answer to whether such a solution could exist is beyond the scope of the present paper. However, we will give next section an argument against such a possibility, based on the physics that leads to this critical situation.

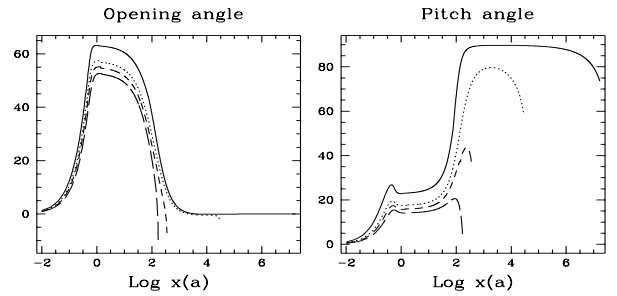


Fig. 7. Jet opening angle ($\theta = \arcsin(B_r/B_z)$, left pannel) and pitch angle ($\arctan(-B_\phi/B_p)$, right pannel) in degrees, for $\varepsilon = 10^{-2}$, $\alpha_m = 1$ and $\xi = 0.005$ (solid line), 0.01 (dotted line), 0.02 (short-dashed line) and 0.05 (long-dashed line). The jet opening angle is positive when the jet widens, negative when it undergoes a recollimation. While jets with high ejection indices refocus with an angle of order -10° , the others are almost cylindrical, with an angle smaller than 1° (but negative).

Note that all jets displayed here achieve a super fast-magnetosonic poloidal speed, namely an usual fast-magnetosonic Mach number $n^2 = u_p^2/V_{FM}^2 > 1$. The last critical point ($t^2 = 1$) would in principle constrain another parameter of the MAES (e.g. the ejection index ξ), thus leaving free (but severely bracketed) mostly one parameter, the disc aspect ratio ε (α_m is supposed to be provided by calculations of MHD turbulence inside the disc).

Recollimation of magnetic surfaces is an old result: all BP82’s solutions displayed such a “turning radius”, while PP92 found that such a behaviour could be generic for cold jets (they did not use any self-similar ansatz). Contopoulos & Lovelace (1994) however, using also a self-similar ansatz, obtained jets with different asymptotic behaviours: recollimating, ever-widening and oscillating. But these solutions were obtained by varying the magnetic configuration parameter (β) independently from the others (λ and κ) and so, cannot describe jets from Keplerian discs. These different behaviours reflect the richness of the equations governing MHD jets.

Following PP92, let us define $\chi = m^2 r_A^2 / r^2$ as a measure of the jet widening. At the turning point ($B_r^t = 0$), Bernoulli equation writes

$$\chi_t^2 \simeq \alpha_t^2 \kappa^2 \lambda^2 , \quad (53)$$

which, in the limit $g_t \simeq 1$, provides the cubic

$$\chi_t^3 - (2\lambda - 3)\kappa^2 \lambda^2 (\chi_t - 1) \simeq 0 . \quad (54)$$

In that limit, one has $\chi = n^2/2 - 1$ (PP92). Solving the cubic and using this last expression, allows us to show that jets will recollimate when they reach

$$n^2 > n_t^2 = 2\kappa\lambda(2\lambda - 3)^{1/2} - 3 . \quad (55)$$

In the other limiting case ($g_t \simeq 0$), Eq.(53) provides directly the condition

$$n^2 > n_t^2 = \kappa\lambda(\lambda - 3)^{1/2} . \quad (56)$$

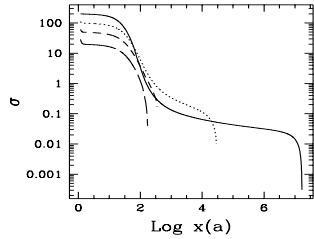


Fig. 8. Ratio σ of the Poynting flux to the kinetic energy flux, logarithm of the Alfvénic Mach number m^2 , total current I flowing within the magnetic surface (normalized to the current I_{ISM} provided at the jet basis), and logarithm of the jet density along any magnetic surface, for various ejection indices. These curves were obtained for the same parameters as in Fig. 7. The jet density is normalized to the disc midplane density $\rho_o = \dot{M}_a(r_o)/8\pi q\mu\varepsilon^2\Omega_o r_o^3$, at the radius r_o . The jet acceleration depends on how much a magnetic surface widens ($m^2 = \rho_A/\rho$), which is possible only if the current decreases. Here, this acceleration is very efficient, the magnetic structure feeding plasma with almost all its power ($\sigma \ll 1$).

Both criteria, similar to those found by BP82 and PP92, are indeed verified numerically for extreme cases (all solutions have $n^2 > 1$). However, we used only Bernoulli equation to derive them: it is the jet transverse equilibrium that will tell us whether or not such a possibility is indeed verified. Thus, we haven't provided yet a satisfactory answer to why do jets recollimate.

5.2. Why do self-similar jets from Keplerian discs always recollimate?

In order to understand what forces the jet to bend towards the axis, one can fruitfully look at another form of the jet transverse equilibrium equation (20), namely

$$(1 - m^2) \frac{B_p^2}{\mu_o \mathcal{R}} - \nabla_{\perp} \left(P + \frac{B^2}{2\mu_o} \right) - \rho \nabla_{\perp} \Phi_G + (\rho \Omega^2 r - \frac{B_{\phi}^2}{\mu_o r}) \nabla_{\perp} r = 0 \quad (57)$$

where $\nabla_{\perp} \equiv \nabla a \cdot \nabla / |\nabla a|$ provides the gradient of a quantity perpendicular to a magnetic surface ($\nabla_{\perp} Q < 0$ for a quantity Q decreasing with increasing magnetic flux) and \mathcal{R} , defined by

$$\frac{1}{\mathcal{R}} \equiv \frac{\nabla a}{|\nabla a|} \cdot \frac{(\mathbf{B}_p \cdot \nabla) \mathbf{B}_p}{B_p^2}, \quad (58)$$

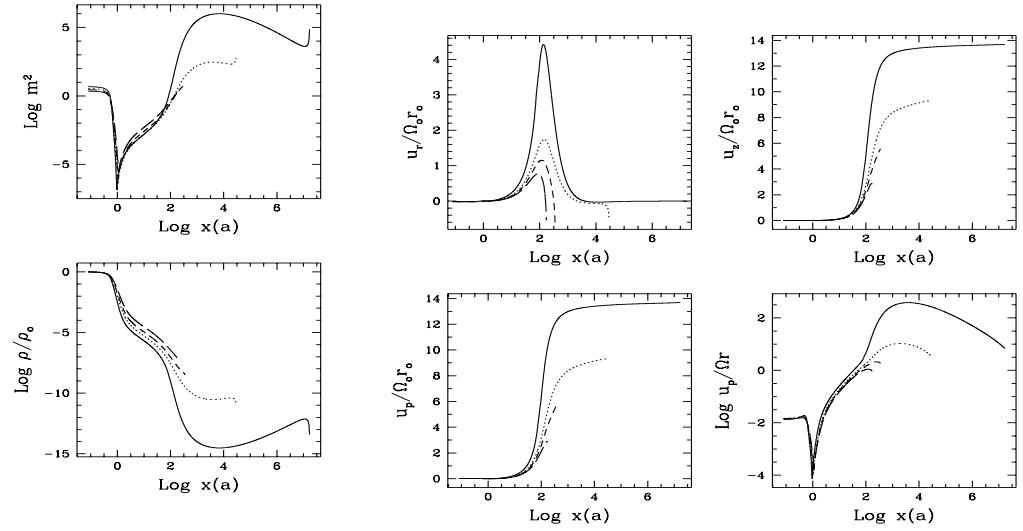


Fig. 9. Components of the jet poloidal velocity u_p and logarithm of the ratio of the poloidal to the azimuthal velocity, measured along a magnetic surface for various ejection indices (see Fig. 7). For these typical solutions, the jet always reaches its maximum velocity (see text), mainly as a vertical component. For small ejection indices, a full relativistic treatment should be used for jets around compact objects. Inside the disc, matter is being accreted with a velocity of order ε the Keplerian velocity. The turning point ($u_r = 0$) occurs roughly at the disc surface ($x = 1$, see FP95).

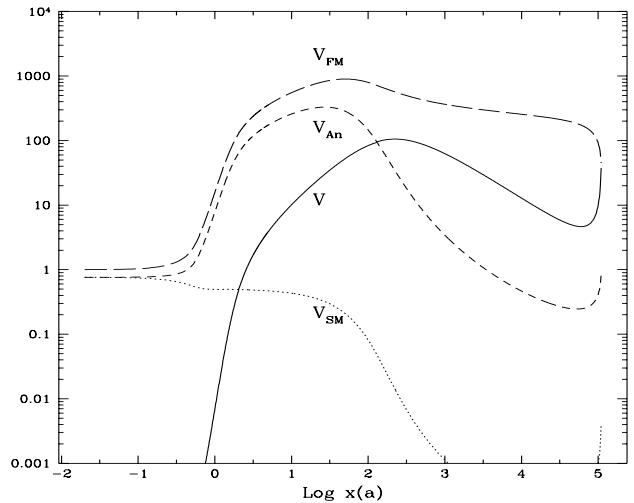


Fig. 10. Characteristic velocities in units of the disc sound speed $\Omega_o h_o$ for $\xi = 0.009$, when $\varepsilon = 10^{-2}$, $\alpha_m = 1$. The jet becomes super-SM slightly above the disc, meets the Alfvén surface at $z_A \simeq 9.6r_o$, where r_o is the field line anchoring radius on the disc, and finally stops when it meets the FM critical surface. See FP95 for the expressions of these critical velocities; in particular, $V = n \cdot u$ is not the jet poloidal velocity.

is the local curvature radius of a particular magnetic surface (Appl & Camenzind 1993a). When $\mathcal{R} > 0$, the surface is bent outwardly while for $\mathcal{R} < 0$, it bends inwardly. The first term in Eq.(57) describes the reaction to the other forces of both magnetic tension due to the magnetic surface (with the sign of the curvature radius) and inertia of matter flowing along it (hence with opposite sign). The other forces are the total pressure gradient, gravity (which acts to close the surfaces and decelerate the flow, but whose effect is already negligible at the Alfvén surface), and the centrifugal outward effect competing with the inwards hoop-stress due to the toroidal field (Fig. 11).

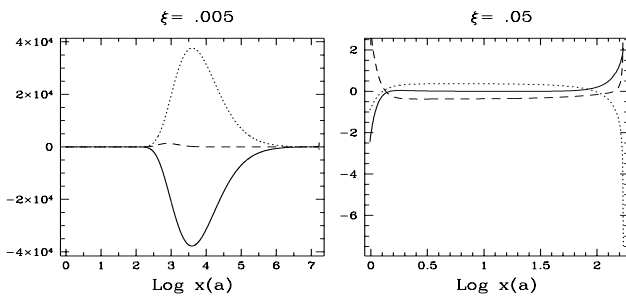


Fig. 11. Forces perpendicular to a given magnetic surface, along it, in units of $B_p^2/\mu_0 r$, for $\alpha_m = 1$, $\varepsilon = 0.01$ and $\xi = 0.005$ (left), $\xi = 0.05$ (right). The solid line is the sum of gravitational, centrifugal and hoop-stress, the dotted line is the total pressure gradient and the dashed line is the magnetic structure response (namely, the term $(1 - m^2)r/\mathcal{R}$). Confining forces are negative. In the high- ω_A limit (left), it is the hoop-stress that is responsible for recollimation ($\log x_A = 1.92$, $\log x_t = 3.6$). In the low- ω_A limit (right), it is the pressure gradient associated to the poloidal field ($\log x_A = 2.1$, $\log x_t = 2.2$).

For current-carrying jets (high ω_A , $g_A \lesssim 1$), recollimation occurs because of the constriction effect of the toroidal magnetic field (as first discovered by BP82). For such highly super-Alfvénic solutions, the jet transverse equilibrium depends mostly on the balance between this force and the centrifugal one. Therefore, it will undergo recollimation only if the jet widens enough and reaches the cylindrical radius

$$\frac{r_t}{r_o} \simeq \zeta_t^{-1/2} \kappa^{1/2} \lambda (2\lambda - 3)^{1/4}. \quad (59)$$

where

$$\zeta_t \equiv \left(\frac{\nabla_{\perp} \ln I}{\nabla_{\perp} \ln r} \right)_t = \beta - 1 - \left(\frac{\partial \ln B_{\phi}}{\partial \ln x} \right)_t \quad (60)$$

describes how strongly the current varies across the magnetic surfaces at (z_t, r_t) . In the expression of the turning radius, the other term scales as $\xi^{-3/4}$, implying that for smaller ejection indices, the jet must open more in order to reach r_t . However, Fig. 6 shows that r_t increases with

ξ much quicker than $\xi^{-3/4}$. Thus, ζ_t plays an important role and decreases very rapidly with ξ : we found numerically that for $\varepsilon = 0.01$, $\alpha_m = 1$, we get $\zeta_t \simeq 1, 10^{-1}, 10^{-4}$ for $\xi = 0.015, 0.01, 0.005$ respectively. In fact, ζ_t is more generally a function of the fastness parameter ω_A (which increases for decreasing ξ): the faster the “rotator” and the bigger the maximum radius reached (see Fig. 12). The centrifugal picture is therefore quite appealing here, but one should not forget that ω_A is a measure of I_A .

For current-free jets (low ω_A , $g_A \ll 1$), $r_t \gtrsim r_A$ and the flow is only slightly super-Alfvénic. Here, the ratio of the toroidal magnetic force to the centrifugal one writes

$$\frac{B_{\phi}^2}{\mu_0 \rho \Omega^2 r^2} \frac{\nabla_{\perp} \ln I}{\nabla_{\perp} \ln r} \simeq \zeta_t g_t^2 \quad (61)$$

with ζ_t of order unity but $g_t \ll 1$. Thus, the force responsible for recollimation can only be the magnetic pressure gradient associated with the poloidal field. Indeed, the jet transverse equilibrium (57) implies that this force is negative, hence trying to close the jet. If both centrifugal force and magnetic force associated to the toroidal field cannot overcome it, the jet cannot avoid a recollimation (Fig. 11). If $\omega_A > 1$ is a necessary condition to obtain trans-Alfvénic jets, it is obviously not sufficient: the “rotator” must be fast enough to allow the propagation of jets much farther away from the Alfvén surface. Since this result appears at the Alfvén surface vicinity, we believe that it is real, namely independent of our self-similar modelling.

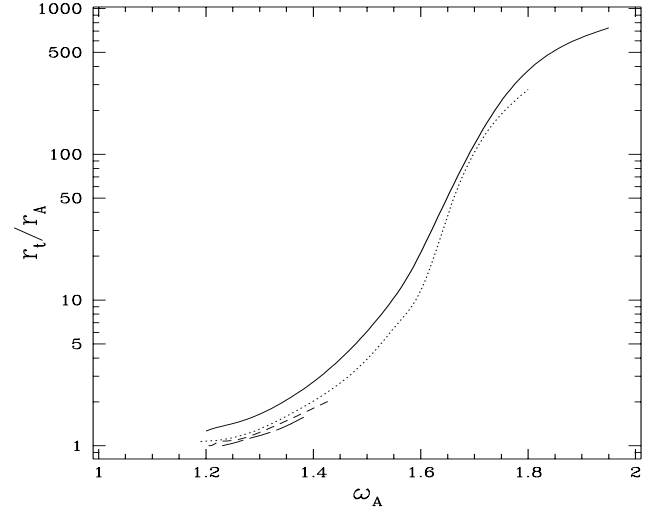


Fig. 12. Ratio of the maximum radius achieved r_t to the Alfvén radius, as a function of the fastness parameter ω_A , for $\alpha_m = 1$ and $\varepsilon = 10^{-1}$ (solid line), 10^{-2} (dotted line), 10^{-3} (short-dashed line), $7 \cdot 10^{-4}$ (long-dashed line). Regularity conditions at SM and Alfvén points fix the range of allowed ω_A . The jet is extremely sensitive to this parameter: jets with $1 < \omega_A < 1.5$ reach only a few times the Alfvén radius before undergoing recollimation.

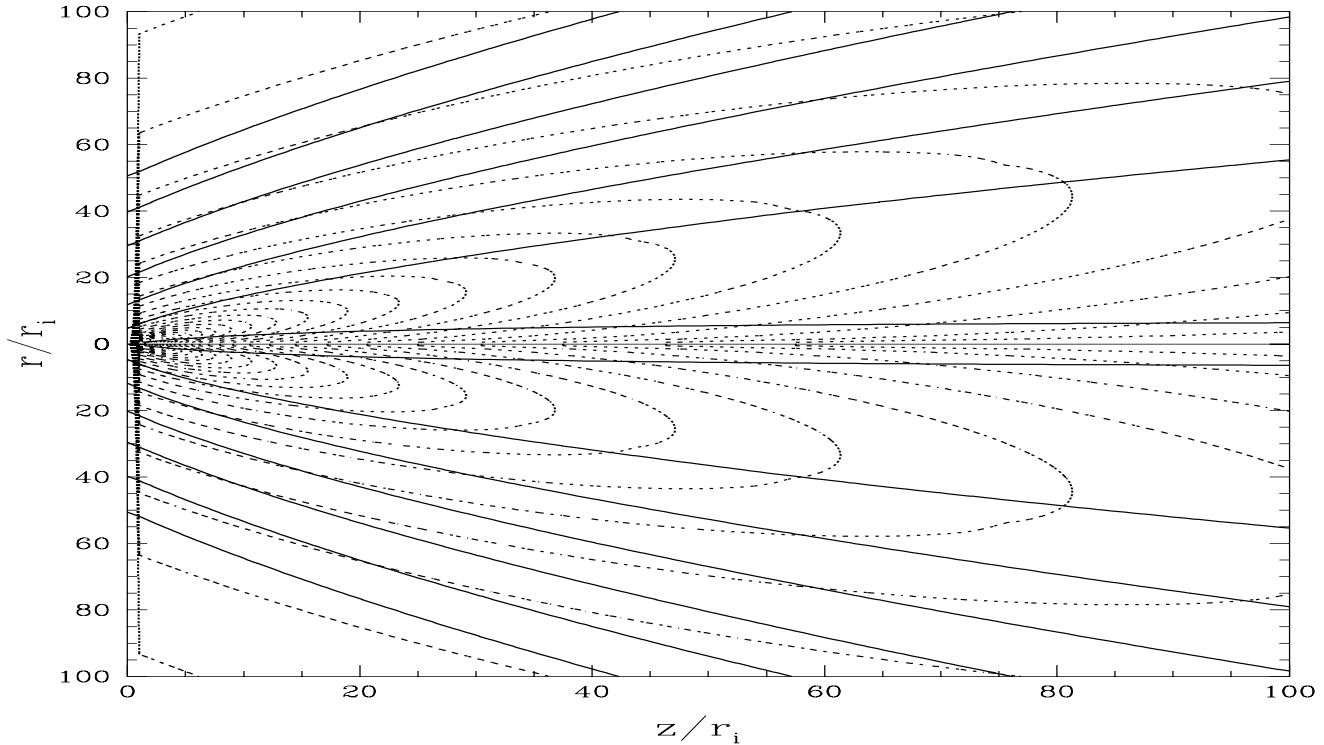


Fig. 13. Isocontours of poloidal current density (J_p , dotted lines) and poloidal magnetic field lines (B_p , solid lines) for a cold jet with $\xi = 0.01$, launched from a disc of $\varepsilon = 10^{-2}$, $\alpha_m = 1$. The current circuit displays a butterfly-like shape, characteristic of tenuous ejections ($\xi < 1/2$). The current flows down the jet axis, enters the disc at its inner edge r_i and returns along the jet itself. Force-free solutions would have $J_p \parallel B_p$, which is not quite achieved here, even for smaller values of ξ . The jet carries its own current, building up a global electric circuit as it propagates through the interstellar medium.

We can now try to understand the fate of cold jets from Keplerian discs, once they start to recollimate. At the turning radius, matter has almost reached its maximum poloidal velocity, with $n^2 \gg 1$ (for high ω_A jets). There is therefore no way to slow down the poloidal motion (F_\parallel remains too small) and, despite the decrease in the jet radius (leading to a decrease in $m^2 = \rho_A/\rho$), the poloidal velocity remains roughly constant. Matter carries away the field with it, strongly decreasing the jet pitch angle. Thus, the total current I (or equivalently B_ϕ) goes to zero. Eventually, the dominant magnetic pressure effect in Eq.(57) becomes the one due to the poloidal field. Because of recollimation, the pressure gradient associated with the poloidal field changes its sign and pinches the jet too (some sort of depression). As a result, the jet is forced to bend towards the axis, with a curvature radius \mathcal{R} becoming infinitely negative. This behaviour was also obtained by Contopoulos & Lovelace (1994) and lead these authors to propose that the assumption of steady-state should break down at these distances. More generally, any steady-state jet with zero poloidal current would be asymptotically parabolic (Heyvaerts & Norman 1989). Such a situation is very far from the actual recollimating regime. Thus, it seems reasonable to guess that stationarity breaks down at the jet

“end” (where $t^2 = 1$ is met but not crossed) and that a shock is formed there.

It is interesting to note that, although they used the same self-similarity ansatz as we did, Contopoulos & Lovelace (1994) found also non-recollimating (for $\beta < 1$) and oscillating (for $\beta > 1$) solutions. But, as already said, those were obtained with parameters that do not correspond to disc-driven jets and achieved regimes with $n^2 < 1$, thereby allowing a different asymptotic state. On the same line of thought, any neglect of the poloidal field (like in Contopoulos 1995) would miss the magnetic depression effect due to recollimation, hence modifying also the jet asymptotic equilibrium (and possibly allowing trans-FM solutions by fine-tuning a parameter).

5.3. Why do self-similar jets widen so much ?

For current-carrying jets (Fig. 13), it has been shown that jets recollimate through the constriction action of the magnetic field. This is possible because the jet radius keeps on opening, allowing a huge acceleration efficiency as well as a decrease of the matter rotation rate. Why do we obtain such a systematic behaviour ?

To address this question, it is worthwhile to look at the Grad-Shafranov equation (20), written in the following form

$$(1 - m^2)J_\phi = J_\lambda + J_\kappa . \quad (62)$$

It expresses that the toroidal current is generated by two main sources, namely

$$J_\lambda = \rho r \left\{ \frac{d\mathcal{E}}{da} + (1 - g)\Omega_* r^2 \frac{d\Omega_*}{da} + g\Omega_* \frac{d\Omega_* r_A^2}{da} \right\} \quad (63)$$

that depends mostly on how the magnetic lever arm behaves from one magnetic surface to another, and

$$J_\kappa = m^2 \frac{\nabla a}{\mu_0 r} \cdot \nabla \ln \rho + r \frac{B_\phi^2 - m^2 B_p^2}{2\mu_0} \frac{d \ln \rho_A}{da} \quad (64)$$

strongly dependent on the mass load at each surface. It is clear that the behaviour of global quantities has a tremendous importance on the jet equilibrium, thus casting doubts on approaches that are not truly 2-D. In the self-similar description of disc-driven jets and within our parameter range, one always achieves a turning point ($B_r^t = 0$) with $\sigma_t \ll 1$. Since the toroidal current at this point,

$$J_\phi^t \simeq -\frac{1}{\mu_0} \frac{\partial B_z}{\partial r} \propto \beta(2 - \beta) \quad (65)$$

is positive, recollimation is allowed only if the currents J_κ^t or J_λ^t are negative. At this turning point, one source writes

$$J_\kappa^t \simeq \frac{B_p^2 r}{2\mu_0 B_o r_o^2} \left\{ \frac{B_\phi^2}{B_p^2} \left(\frac{d \ln \rho_o}{d \ln r_o} + \frac{d \ln \rho_A / \rho_o}{d \ln r_o} \right) + m^2 \left(\frac{d \ln \rho_o}{d \ln r_o} - \frac{d \ln \rho_A / \rho_o}{d \ln r_o} \right) \right\} , \quad (66)$$

for all solutions. On the contrary, the other current source strongly depends on g (thus on ω_A): for $g_t \simeq 1$ it writes

$$J_\lambda^t \simeq \frac{\rho \Omega_o^2 r}{2B_o} \left\{ 3 + 2\lambda \left(\frac{d \ln \lambda}{d \ln r_o} - 1 \right) \right\} \quad (67)$$

and for $g_t \simeq 0$

$$J_\lambda^t \simeq \frac{\rho \Omega_o^2 r}{2B_o} \{ 3 - 3\lambda \} . \quad (68)$$

Self-similar solutions necessarily imply that ratios like r_A/r_o and ρ_A/ρ_o are constant through all the jet. Their logarithmic derivatives are therefore zero and both current sources are indeed negative at the turning point ($d \ln \rho_o / d \ln r_o = 2\beta - 3 = -3/2 + \xi < 0$, FP93a). Thus, our systematic behaviour arises from both our MAES parameter space and the fulfilment of this condition. On the contrary, any jet with $g_t \sim 1$ (high ω_A) but satisfying

$$\begin{aligned} \frac{d \ln r_A / r_o}{d \ln r_o} &> \frac{1}{2} \\ \frac{d \ln \rho_A / \rho_o}{d \ln r_o} &< \frac{d \ln \rho_o}{d \ln r_o} \end{aligned} \quad (69)$$

would never allow $J_\phi^t > 0$ and therefore, would not undergo recollimation. This sufficient condition expresses that high- ω_A jets would not widen so much as they do here, the magnetic structure keeping stored a significant amount of the power provided by the disc. Since our parameter space is only slightly dependent on our self-similar modelling, we claim that it describes realistic boundary conditions for any given magnetic surface. Therefore, we expect that any model of a magnetically-driven jet would also undergo recollimation if conditions (69) are not met. “Over-widening” and then recollimation would be general features, independent on the analytical model used, of cold jets from discs described by constant parameters. This is consistent with PP92, who did not use any self-similar assumption, but found recollimating solutions by making the approximation ω_A (their λ parameter) constant through the jet. Sakurai (1987) performed full numerical simulations of jets from accretion discs that crossed the three usual critical points (measured with the poloidal velocity), but without taking self-consistently into account the disc. Because of the limited computational domain, it is difficult to figure out whether or not his solutions display a recollimation (see the vertical scale involved for small ξ in Fig.6). However, his initial split-monopole geometry for the magnetic configuration forbids the development of a jet with a constant ξ (see his Fig.3). To determine if the final configuration is realistic would require a full 2-D treatment of the disc-jet interrelations.

For current-free or low- ω_A jets ($g_t \sim 0$), non-recollimating solutions could in principle be obtained if

$$\frac{d \ln \rho_A / \rho_o}{d \ln r_o} < \frac{d \ln \rho_o}{d \ln r_o} - 3 \frac{\lambda - 1}{\lambda - 3} \quad (70)$$

is verified. This necessary condition is much more stringent than in the case of high- ω_A jets, and we have strong doubts that it could ever be met. As already mentioned however, we expect that the behaviour of these kind of jets is mostly independent of our modelling.

It is noteworthy that differential rotation is of so great importance for both jet formation and collimation. Indeed, it has already been found that without the counter current due to the disc differential rotation, no magnetically-driven jet could be possible. Here, we find that in the absence of differential rotation ($d\Omega_*/da = 0$), one of the two sources of toroidal current remains positive for any g_t , namely

$$J_\lambda^t \simeq \frac{\rho \Omega_o^2 r}{2B_o} \left\{ 3 + g_t \lambda \left(4 + 2 \frac{d \ln \lambda}{d \ln r_o} \right) \right\} . \quad (71)$$

Thus, differential rotation of magnetic surfaces has a tremendous importance in recollimating outflows, or more generally, in their asymptotic behaviour. This is a very important effect and shows that jets from a rigidly rotating object (e.g., a star) will certainly have a different asymptotic behaviour than jets from accretion discs. In partic-

ular, they can display non-recollimating or oscillating behaviours (Tsinganos & Trussoni 1991, Sauty & Tsinganos 1994).

MAES are expected to be settled in the innermost part of a larger accretion disc, where both the energy reservoir and magnetic field strength are bigger. Such a picture implies that a viscous-like transport of angular momentum acts in the outer disc until magnetic braking due to the jet overcomes it in the inner regions. One would then obtain a transition, as r_o decreases, from $\xi = 0$ to $\xi \lesssim 0.01$ with the corresponding changes in r_A/r_o (from infinity to a finite value) and ρ_A/ρ_o (from zero to a finite value). Thus, the conditions (69) could be naturally fulfilled in a self-consistent picture taking into account realistic boundary conditions. Needless to say that only 2-D numerical calculations could achieve it.

6. Summary and conclusion

In this paper, we have covered all dynamical processes at work in a stationary, weakly dissipative MAES of bipolar topology (see Appendix A for quadrupolar), by constructing continuous solutions from the accretion disc to super-Alfvénic jets. We summarize below our findings and discuss their implications.

(1) We have demonstrated that the usual parameters for magnetically-driven (cold) jets, namely the magnetic configuration, lever arm and mass load, are intrinsically related to the disc ejection efficiency ξ . Thus, realistic jets would be described by a distribution of ξ with the magnetic surfaces (or their anchoring radius).

(2) We showed that this parameter lies in a very narrow range for cold jets, namely $0.004 \lesssim \xi \lesssim 0.08$. A minimum ejection efficiency is required for the disc to find a quasi-MHS equilibrium. A crude modelling of this sensitive equilibrium leads most probably to unstable regimes, the disc being too much pinched by the Lorentz force. On the other hand, a maximum mass load arises from the constraint of accelerating matter up to super-Alfvénic speeds. The threshold for the minimum ejection index is raised for decreasing disc aspect ratio ε and turbulence parameter α_m . Both constraints impose that these parameters must verify $0.0005 < \varepsilon \leq 0.1$ and $0.1 < \alpha_m \leq 1$.

(3) As a result, the current must enter the disc at its inner edge, flow back in the jet and close by flowing down along the axis. This has two important consequences. First, although the disc can afford larger ejection efficiencies (Ferreira 1994), they would be non-steady, the flow not being able to reach the Alfvén surface. Second, this implies a strong influence on what's going on at the axis, thus suggesting a coupling with the inner central object magnetosphere. This work is under progress.

(4) The existence of a minimum ejection index has strong implications on jet energetics. Indeed, it forbids to construct jet models where the mass load is arbitrarily small (and thus, an asymptotic velocity arbitrarily high).

Nevertheless, in the range allowed for ξ , the ratio of the total ejection rate (in one jet) to the accretion rate, $f \equiv \dot{M}_{je}/\dot{M}_{ac}$, would vary between 10^{-3} and 10^{-1} , depending on both ξ and the radial extension r_e/r_i of the magnetized disc (Ferreira 1996). This is in complete agreement with recent estimates made by Hartigan et al. (1995), who find a typical value of 10^{-2} for jets from young stars.

The jet magnetization parameter (Michel 1969, Camenzind 1987),

$$\sigma_* \equiv \frac{\Omega_*^2 B_o r_o^2}{\eta c^3} = 6.8 \left(\frac{\sigma_{SM}}{100} \right) \left(\frac{-B_o}{2B_{\phi,SM}} \right) \left(\frac{r_o}{3r_g} \right)^{-3/2} \quad (72)$$

shows that relativistic jets could be possible around compact objects. If Compton drag can be avoided (Phinney 1987), the mean bulk Lorentz factor $\bar{\gamma}$ that such jets could achieve,

$$\bar{\gamma} = 1 + \frac{\eta_{lib}}{24f} (1 + \bar{\sigma}_\infty)^{-1} \left(\frac{r_i}{3r_g} \right)^{-1} \quad (73)$$

strongly depends on how much power the magnetic structure keeps stored in its asymptotic regime (see FP95 for the definition of η_{lib}). As an example, for $\bar{\sigma}_\infty = 1$ (final kinetic energy flux comparable to the Poynting flux, Li et al. 1992), one gets $\bar{\gamma}$ between 1 ($\xi = 0.07$, $r_e = 100r_i$) and 8 ($\xi = 0.004$, $r_e = 2r_i$), with typical values lying between 1 and 4. Thus moderate mean bulk Lorentz factors are likely to be achieved by cold jets from compact objects.

In the context of YSOs, the mean jet velocity writes

$$\bar{u}_\infty = \Omega_i r_i (1 + \bar{\sigma}_\infty)^{-1/2} \left(\frac{\eta_{lib}}{2f} \right)^{1/2}, \quad (74)$$

where $\Omega_i r_i$ is the angular velocity at the inner disc radius. For $\bar{\sigma}_\infty = 1$, jets can reach a velocity between 1 ($\xi = 0.07$, $r_e = 100r_i$) and 10 ($\xi = 0.004$, $r_e = 2r_i$) times this velocity, with typical factors between 2 and 6. For structures settled at $r_i \simeq 30r_\odot$ (10 stellar radii for a typical T-Tauri star), this provides jets with a mean velocity between 100 and 500 km s^{-1} , in agreement with observations.

(5) All the above results are general to magnetically-driven jets from Keplerian accretion discs. We constructed global solutions, from the accretion disc to a super-Alfvénic jet, using a self-similar ansatz. It has been shown that the jet asymptotic behaviour strongly depends on the fastness parameter ω_A , which describes how fast is the magnetic “rotator” and is a measure of the amount of current still available at the Alfvén surface. This parameter must be bigger than (but of the order of) unity and is very sensitive to the physical conditions inside the disc. All our solutions display the same behaviour: the jet widens until a very strong acceleration efficiency is achieved, all the available power being eventually transferred into kinetic power; the centrifugal force decreases so much that the Lorentz force pinches the jet, making it to recollimate. The bigger ω_A and the larger the maximum radius reached

by the jet. Inside our parameter range (which is weakly affected by our self-similar assumption), this behaviour stems from having a constant ejection index ξ . Therefore, we expect that non self-similar jets from Keplerian discs described with constant parameters would also display recollimation, unless realistic 2-D boundary conditions are taken into account. Such boundaries should concern the transition from the outer viscous disc to the inner magnetized one, as well as a possible interaction with the central object.

(6) If magnetized discs are driving jets over a wide range of radii, then they can probably be described by an almost constant ejection index ξ (and self-similar solutions are not too bad an approximation). In those circumstances, one would expect that these jets undergo a recollimation and then a shock, making the whole structure unsteady. Whether or not such a shock is terminal or a “magnetic focal point” (Gomez de Castro & Pudritz 1993, Ouyed & Pudritz 1993) remains to be carefully worked out. Besides the shock signature, such a structure could be detected through its apparent lack of radiation coming from the magnetized disc itself (FP95). However, one has to bear in mind that the fate of jets could be strongly modified by the external medium (Appl & Camenzind 1993a). Indeed, an external confinement could forbid a natural “over-widening”, thus enforcing a redistribution of the current density inside the jet. By this way, asymptotic solutions with $\nabla_{\parallel} I = 0$ but with non-vanishing current I (in contrast with what is obtained here) could perhaps be achieved. Such an hypothesis should deserve further investigation.

(7) Finally, a major challenge remains the question of the source for the required magnetic diffusivity. Indeed, Heyvaerts et al. (1996) showed that in a disc braked by viscous stresses, any instability (possibly magnetic), triggering a turbulence with an injection scale of order the disc thickness, would provide $\mathcal{R}_m \sim 1$. Such a situation is therefore incompatible with magnetically-driven jets. As a consequence, these powerful jets require physical conditions that were not yet investigated in discs like those, for example, met at the interaction with the central object magnetosphere. On the other hand, thermally-driven jets (but magnetically confined) should be viewed as a possible alternative. The jet power could be reduced down to a level comparable to the disc luminosity (see Eq.(14), with $\Lambda \sim 1$). Such a picture is appealing because it allows jets along with radiating discs and offers a smooth transition between “viscous-like” discs and MAES (Ferreira, in preparation).

Acknowledgements. I would like to thank the referee, Kanaris Tsinganos, for his helpful comments, as well as Max Camenzind, Jean Heyvaerts, Stefan Appl, Ramon Khanna and Guy Pelletier for enthusiastic and stimulating discussions. This work was supported by the Deutsche Forschungsgemeinschaft (SFB 328).

A. Appendix: Quadrupolar topology and the production of jets

In this appendix, we briefly investigate the structure of a Keplerian accretion disc, threaded by a large scale magnetic field of quadrupolar topology. Such a topology is described by an even toroidal field and a magnetic flux $a(r, z)$ (see Eq.(6)), being an odd function of z . The magnetic field inside the disc follows the plasma, with $B_{z,o} = 0$, $B_{r,o} < 0$ and $B_{\phi,o} > 0$ (subscripts “o” refer to quantities at the disc midplane). Since both plasma angular velocity and poloidal magnetic field increase towards the center (we don’t take into account a possible boundary layer between the disc and the central object), the disc can be divided into two distinct regions (see Lovelace et al. 1987, Khanna & Camenzind 1992). The inner region is characterized by a positive vertical current density at the disc midplane ($J_{z,o} > 0$), but negative at its surface ($J_z^+ < 0$). The outer region displays the opposite behaviour, with $J_{z,o} < 0$ and $J_z^+ > 0$ (the transition between the two is of course at the radius where $J_{z,o} = 0$).

One would like to build up a Keplerian disc (that is, in quasi-MHS equilibrium in both radial and vertical directions), accreting towards the center ($u_{r,o} < 0$) and giving rise to a magnetically propelled jet. This last demand requires the following (necessary) conditions: (a) open field lines (B_z^+ and B_r^+ both positive), (b) a positive MHD Poynting flux (for $z > 0$, namely $B_{\phi}^+ < 0$) and (c) a MHD acceleration ($\nabla_{\parallel} I > 0$, see Eq.(15)).

The inner region is unable to steadily produce MHD jets. This arises from the topology itself, which provides $F_{\phi}^+ < 0$ (therefore $F_{\parallel} < 0$): the magnetic structure would slow down any plasma that could have been (thermally) ejected out from the underlying disc.

On the contrary, the outer region can in principle produce jets. Let us then examine its structure. Since the Lorentz force is accelerating the matter at the disc midplane, accretion is achieved only if the viscous torque is dominant ($\Lambda < 1$). Thus, the accretion velocity is

$$u_o = -u_{r,o} \simeq 2(1 - \Lambda) \frac{\nu_{v,o}}{r}, \quad (A1)$$

where $\nu_{v,o}$ is the anomalous viscosity (measured at the disc midplane). Both radial and vertical components of the Lorentz force are positive, thus counter-acting gravity inside the disc. If the disc is in quasi-MHS vertical equilibrium, then the deviation from Keplerian rotation law is of the order ε^2 . At the disc surface, the vertical Lorentz force changes its sign, keeping nevertheless $F_{\parallel} > 0$ if $J_z^+ > J_r^+ B_z^+ / B_r^+$ is satisfied (condition (c)), with $J_r^+ > 0$. Condition (a) is fulfilled at the disc surface only if the vertical scale of variation of the magnetic flux is of the order of the disc scale height. Steady-state diffusion of the poloidal field (Eq.(4)) requires then a “poloidal” magnetic diffusivity such that $\nu_{m,o} \simeq \varepsilon u_o h$. The toroidal field at the disc surface can be written as $B_{\phi}^+ = B_{\phi,o} + B_{\phi}^{\nabla \Omega}$, where

$B_\phi^{\nabla\Omega}$ is provided by the disc differential rotation (Eq.(5)). Since B_ϕ^+ must be negative (condition (b)),

$$\frac{B_{\phi o}}{-B_{ro}} \lesssim \frac{3}{2} \frac{\Omega_o r}{u_o} \frac{\nu_{m,o}}{\nu'_{m,o}} \quad (\text{A2})$$

where $\nu'_{m,o}$ is the “toroidal” diffusivity (see Sect. 2.1). With these estimates, one obtains that with the following restrictions, namely

$$\begin{aligned} \frac{B_{r,o}^2}{\mu_o P_o} &\simeq \Lambda^2 \left(\frac{\nu_{v,o}}{\Omega_o h^2} \right)^2 \\ \frac{B_{\phi,o}^2}{\mu_o P_o} &< 1 \\ \frac{\nu_{m,o}}{\nu'_{m,o}} &\lesssim \frac{4}{3} (1 - \Lambda) \frac{\varepsilon^2}{\Lambda} \\ \frac{\nu_{m,o}}{\nu_{v,o}} &\simeq 2(1 - \Lambda) \varepsilon^2 \end{aligned} \quad (\text{A3})$$

where $\Lambda < 1$ and the plasma pressure $P_o = \rho_o \Omega_o^2 h^2$ (quasi-MHS vertical equilibrium), quadrupolar topologies fulfill the disc requirements as well as the jet conditions (a) and (b) (condition (c) requires a full calculation of the vertical structure). Note that above the disc surface, the current system is similar to the one of a bipolar magnetic topology: the magnetic energy that feeds the jet arises from the disc plasma itself, extracted where $F_\phi < 0$ (in a layer around $J_z = 0$). Since the torque there cannot be as strong as in the bipolar case, one gets the general result that jets from quadrupolar topologies would be weaker.

However, this configuration demands very peculiar conditions on the disc turbulence. Indeed, a situation giving rise to $\Lambda \lesssim 1$ requires $\nu_m \sim (1 - \Lambda) \varepsilon^2 \nu'_m$ with $\nu'_m \sim \nu_v$, whereas $\Lambda \sim \varepsilon$ is achieved for $\nu_m \sim \varepsilon \nu'_m \sim \varepsilon^2 \nu_v$, and $\Lambda \sim \varepsilon^2$ for $\nu_m \sim \nu'_m \sim \varepsilon^2 \nu_v$. Such a situation is against our current understanding of turbulence, where all transport coefficients should achieve a comparable level (Pouquet et al. 1976). Therefore, it is dubious that such a topology could produce MHD jets. It could nevertheless play a role in a quadrupolar “cored apple” circulation around protostellar sources (Henriksen & Valls-Gabaud 1994, Fiege & Henriksen 1996).

B. Appendix: Toroidal field at the disc surface

We start with Eq.(30), by making a second order Taylor expansion of all the quantities and neglecting the advection term, and we obtain

$$\frac{\eta'_m J_r}{\eta'_o J_o} \simeq 1 - \Gamma \left(\frac{x^2}{2} + 2 \frac{\Omega_o - \Omega}{3 \Omega_o \mathcal{R}_m \varepsilon^2} \right) \quad (\text{B1})$$

where $\Gamma = 3\nu_o/\alpha_m^2 \nu'_o$ is a measure of the degree of anisotropy of the MHD turbulence inside the disc. The disc radial equilibrium provides the angular velocity $\Omega =$

$\Omega_k(1 + \omega)$, where the deviation from Keplerian rotation law comes mainly from the radial magnetic tension,

$$\omega \simeq -\frac{\mu}{2} \mathcal{R}_m \varepsilon^2 v \quad (\text{B2})$$

with $v \equiv \rho_o/\rho \simeq 1 + v''_o x^2/2$. The above expression shows that, as the density decreases vertically, the magnetic effect increases and the plasma rotates with a lower rate. This gives rise to an enhanced accretion velocity above the disc midplane (and a corresponding source of toroidal current, see Figs. 4, 5 and 8 in FP95). The disc vertical equilibrium provides the density profile, namely

$$v''_o \simeq 1 + \mu q^2 + \mu \mathcal{R}_m^2 \varepsilon^2 \quad (\text{B3})$$

where the first term is the tidal force, the second one is the magnetic pressure due to shear (B_ϕ) and the last one is the magnetic pressure due to curvature (B_r). These three effects are comparable (see Fig. 2). Using that the “toroidal” magnetic resistivity decreases vertically as $\eta'_m = \eta'_o(1 - d_o x^2/2)$, we get

$$\frac{J_r}{J_o} \simeq 1 - \delta \frac{x^2}{2} \quad \text{with} \quad \delta = \Gamma \left(1 + \mu \frac{v''_o}{3} \right) - d_o \quad (\text{B4})$$

and therefore, $B_\phi = B_\phi^{J_o} + B_\phi^{\nabla\Omega}$, where $B_\phi^{J_o} = -q B_{o,x}$ and $B_\phi^{\nabla\Omega} = q B_{o,x} \delta x^3/6$. The toroidal field inside the disc is then mainly measured by $B_\phi = -q B_{o,x} f(x)$, with $f(x) = x(1 - \delta x^2/6)$. Since the magnetic diffusivity decreases on a disc scale height (d_o of order unity), the only way to allow a decrease of J_r on such a scale ($\delta > 0$ and of order unity) is to require $\Gamma \simeq 1$. This is the key factor for ejection (Ferreira & Pelletier 1993b, FP95). This, in turn, implies $f_+ = f(1) \simeq 0.5$ to 1. Such an important result is independent of the diffusivity used, as long as it decreases on a disc scale height.

C. Appendix: Minimum ejection index

The disc is not in a perfect MHS equilibrium, but there is a slight motion towards the disc midplane. From mass conservation, we obtain that this tiny motion is

$$u_z \simeq \varepsilon u_o (\xi - 1) x. \quad (\text{C1})$$

Thus, this velocity increases as ξ diminishes, describing the basic fact that the plasma pressure gradient is less effective in sustaining the disc against both tidal and magnetic compression. This then implies that v''_o decreases (see Appendix B), which leads to a decrease of δ , hence an increase of B_ϕ at the disc surface (f_+ increases). Now, a look at Eq.(46) shows that a vertical equilibrium will not be achieved for f_+ too high (how high being obtained only by numerical means).

Equation (30), taking into account the advection term, can be written as

$$\frac{\eta'_m J_r}{\eta'_o J_o} \simeq 1 - \Gamma \left(1 + \mu \frac{v''_o}{3} + \frac{2}{3} (\xi - 1) \alpha_m^2 \mathcal{R}_m \varepsilon^2 \right) \frac{x^2}{2}. \quad (\text{C2})$$

This expression shows that inside the disc, where this expansion is valid, the effect of advection is to decrease the radial current density (although this contribution, of order $\alpha_m^2 \varepsilon$, is negligible). On the contrary, above the disc when $u_z > 0$, this term changes its sign and contributes to maintain $J_r > 0$. Eventually, as one goes from the resistive disc to the ideal MHD jet, this term will completely balance the effect of differential rotation. What the above expression shows, is that its influence will start at lower altitudes for higher α_m and ε . Thus, to the highest values of both α_m and ε corresponds the highest value of f_+ , henceforth the smallest ejection index.

References

Abramowicz, M.A., Piran, T., 1980, *ApJ*, 241, L7
 Abramowicz, M.A., Calvani, M., Nobili, L., 1980, *ApJ*, 242, 772
 Appl, S., Camenzind, M., 1993a, *A&A*, 270, 71
 Appl, S., Camenzind, M., 1993b, *A&A*, 274, 699
 Balbus, A.S., Hawley, J.F., 1991, *ApJ*, 376, 214
 Begelman, M.C., Sikora, M., Rees, M.J., 1987, *ApJ*, 313, 689
 Bertout, C., Basri, G., Bouvier, J., 1988, *ApJ*, 330, 350
 Blandford, R.D., Znajek, R.L., 1977, *MNRAS*, 179, 433
 Blandford, R.D., Payne, D.G., 1982, *MNRAS*, 199, 883 (BP82)
 Bregman, J.N., 1990, *A&AR*, 2, 125
 Bridle, H.A., Perley, A.R., 1984, *ARA&A*, 22, 319
 Cabrit, S., Edwards, S., Strom, S.E., Strom, K.M., 1990, *ApJ*, 354, 687
 Camenzind, M., 1986, *A&A*, 156, 137
 Camenzind, M., 1987, *A&A*, 184, 341
 Camenzind, M., 1990, in G. Klare (ed.), *Rev. in Modern Astrophysics*, 3, Springer-Verlag, Berlin
 Canto, J., 1980, *A&A*, 86, 327
 Chan, K.L., Henriksen, R.N., 1980, *ApJ*, 241, 534
 Chiueh, T., Li, Z-Y., Begelman, M.C., 1991, *ApJ*, 377, 462
 Contopoulos, J., Lovelace, R.V.E., 1994, *ApJ*, 429, 139
 Contopoulos, J., 1995, *ApJ*, 450, 616
 Curry, C., Pudritz, R.E., 1995, *ApJ*, 453, 697
 DeCampli, W.M., 1981, *ApJ*, 244, 124
 Fendt, C., Camenzind, M., Appl, S., 1995, *A&A*, 300, 791
 Ferreira, J., Pelletier, G., 1993a, *A&A*, 276, 625 (FP93a)
 Ferreira, J., Pelletier, G., 1993b, *A&A*, 276, 637
 Ferreira, J., 1994, PhD thesis, Paris VII University
 Ferreira, J., Pelletier, G., 1995, *A&A*, 295, 807 (FP95)
 Ferreira, J., 1996, in W. Kundt (ed.), *Jets from Stars and Galactic Nuclei*, Springer-Verlag, Berlin
 Fiege, J.D., Henriksen, R.N., 1996, *ApJ*, in press
 Foglizzo, T., Tagger, M., 1995, *A&A*, 287, 297
 Galeev, A.A., Rosner, R., Vaiana, G.S., 1979, *ApJ*, 229, 318
 Gomez de Castro, A.I., Pudritz, R.E., 1993, *ApJ*, 409, 748
 Hartigan, P., Edwards, S., Ghandour, L., 1995, *ApJ*, 452, 736
 Hartmann, L., MacGregor, K.B., 1982, *ApJ*, 259, 180
 Hartmann, L., Edwards, S., Avrett, E., 1982, *ApJ*, 261, 279
 Henriksen, R.N., Valls-Gabaud, D., 1994, *MNRAS*, 266, 681
 Heyvaerts, J., Norman, C., 1989, *ApJ*, 347, 1055
 Heyvaerts, J.F., Priest, E.R., 1989, *A&A*, 216, 230
 Heyvaerts, J.F., Priest, E.R., Bardou, A., 1996, *ApJ*, submitted
 Khanna, R., Camenzind, M., 1992, *A&A*, 263, 401
 Khanna, R., Camenzind, M., 1994, *ApJ*, 435, L129
 Königl, A., 1986, *Can. J. Phys.*, 64, 362
 Königl, A., 1989, *ApJ*, 342, 208
 Lada, C.J., 1985, *ARA&A*, 23, 267
 Lago, M.T.V.T., 1984, *MNRAS*, 210, 323
 Li, Z-Y., Chiueh, T., Begelman, M.C., 1992, *ApJ*, 394, 459
 Li, Z-Y., 1995, *ApJ*, 444, 848
 Lovelace, R.V.E., Wang, J.C.L., Sulkanen, M.E., 1987, *ApJ*, 315, 504
 Lynden-Bell, D., Pringle, J.E., 1974, *MNRAS*, 168, 603
 Lynden-Bell, D., 1978, *Phys. Scripta*, 17, 185
 Mestel, L., 1968, *MNRAS*, 138, 359
 Michel, F.C., 1969, *ApJ*, 158, 727
 Mirabel, I.F., Rodriguez, L.F., Cordier, B., Paul, J., Lebrun, F., 1992, *Nature*, 358, 215
 Mouschovias, T.Ch., 1991, *ApJ*, 373, 169
 Novikov, I.D., Thorne, K.S., 1973, in C. Dewitt, B. Dewitt (eds.), *Les astres Occlus*, Les Houches, Gordon and Breach, New York
 Ouyed, R., Pudritz, R.E., 1993, *ApJ*, 419, 255
 Padman, R., Lasenby, A.N., Green, D.A., 1991, in P.A. Hughes (ed.), *Beams and Jets in Astrophysics*, Cambridge Univ. Press
 Papaloizou, J.C.B., Pringle, J.E., 1984, *MNRAS*, 208, 721
 Pelletier, G., Pudritz, R.E., 1992, *ApJ*, 394, 117 (PP92)
 Pelletier, G., Ferreira, J., Henri, G., Marcowith, A., 1996, in K.C. Tsinganos (ed.), *Solar & Astrophysical Magnetohydrodynamic Flows*, Kluwer
 Phinney, E.S., 1983, in A. Ferrari and A.G. Pacholczyk (eds.), *Astrophysical jets*, Reidel Publ. Comp., Dordrecht
 Phinney, E.S., 1987, in J.A. Zensus and T.J. Pearson (eds.), *Superluminal Radio Sources*, Cambridge Univ. Press
 Pouquet, A., Frisch, U., Leorat, J., 1976, *J. Fluid Mech.*, 77, 321
 Pudritz, R.E., 1981, *MNRAS*, 195, 897
 Pudritz, R.E., Norman, C.A., 1983, *ApJ*, 274, 677
 Rees, M.J., Begelman, M.C., Blandford, R.D., Phinney, E.S., 1982, *Nature*, 295, 17
 Rosso, F., Pelletier, G., 1994, *A&A*, 287, 325
 Sakurai, T., 1985, *A&A*, 152, 121
 Sakurai, T., 1987, *PASJ*, 39, 821
 Sauty, C., Tsinganos, K., 1994, *A&A*, 287, 893
 Shakura, N.I., Sunyaev, R.A., 1973, *A&A*, 24, 337
 Shu, F., Najita, J., Ostriker, E., Wilkin, F., Ruden, S., Lizano, S., 1994, *ApJ*, 429, 781
 Spruit, H.C., Stehle, R., Papaloizou, J.C.B., 1995, *MNRAS*, 275, 1223
 Tagger, M., Pellat, R., Coroniti, F., 1992, *ApJ*, 393, 708
 Tsinganos, K., 1981, *ApJ*, 245, 764
 Tsinganos, K., Trussoni, E., 1991, *A&A*, 249, 156
 Tsinganos, K., Sauty, C., Surlantzis, G., Trussoni, E., Contopoulos, J., 1996, in K.C. Tsinganos (ed.), *Solar & Astrophysical Magnetohydrodynamic Flows*, Kluwer
 Uchida, Y., Shibata, K., 1985, *PASJ*, 37, 515
 Wardle, M., Königl, A., 1993, *ApJ*, 410, 218
 Weber, E.J., Davis, L., 1967, *ApJ*, 148, 217
 Yoshizawa, A., Yokoi, N., 1993, *ApJ*, 407, 540
 Zurek, W.H., Benz, W., 1986, *ApJ*, 308, 123